MASTERARBEIT | MASTER'S THESIS

Titel | Title

Validation of patient-derived cell-line and organoid model of mucinous ovarian cancer for MEK Inhibitor Trametinib evaluation

verfasst von | submitted by

Sarah Hanna Guttmann BSc

angestrebter akademischer Grad | in partial fulfilment of the requirements for the degree of

Master of Science (MSc)

Wien | Vienna, 2025

Studienkennzahl lt. Studienblatt | Degree programme code as it appears on the student record sheet:	UA 066 865
Studienrichtung lt. Studienblatt | Degree programme as it appears on the student record sheet:	Masterstudium Molecular Biology
Betreut von | Supervisor:	ao. Univ.-Prof. Dr. Dan Cacsire Castillo-Tong

ACKNOWLEDGEMENTS

First, I would like to thank Assoc. Prof. Dan Cacsire Castillo-Tong, Ph.D., for giving me the opportunity to conduct my master thesis internship in her laboratory. Thank you for the insightful scientific advice, the wonderful working climate and overall support. Another huge thank you goes to Akshi Srivastava and Weronika Herc for being wonderful and supportive co-workers during my time in the laboratory. Furthermore, I would like to thank my partner, family and friends for their love and support during my master's degree because without them it would not have been possible.

ABSTRACT

Background: Mucinous ovarian cancer (MOC) is a rare epithelial ovarian cancer subtype with poor prognosis and limited treatment options. Current therapy is derived from high-grade serous ovarian cancer protocols and includes cytoreductive surgery and platinum-based chemotherapy, which show poor efficacy in MOC.

Objectives: The need for suitable preclinical models and effective targeted therapies is still ongoing. Therefore, this thesis aimed to establish a patient-derived cell culture model for drug testing, which was implemented testing the MEK1/2 inhibitor trametinib in MOC. Trametinib was hypothesized to cause antiproliferative effects in cell lines expressing MEK1/2.

Methods: Patient-derived cell lines and corresponding organoids were established to check for resemblance of tumour heterogeneity and architecture in the parent tumours. Trametinib was tested in live-cell imaging, viability, and cytotoxicity assays and compared to the standard chemotherapeutic carboplatin, as well as evaluated for proliferation, apoptosis and target inhibition via IHC staining.

Results: Organoids displayed morphological and immunohistochemical similarity to original tumour tissues, confirming their suitability for drug testing. Trametinib treatment at 10 µM effectively reduced proliferation without inducing pronounced apoptosis, as shown by decreased Ki-67 and unchanged cleaved caspase-3 expression. Loss of the downstream marker c-fos confirmed MAPK pathway inhibition. Drug response varied among cell lines depending on MEK1/2 expression and *KRAS* mutation status.

Conclusion: The findings demonstrate that patient-derived organoids faithfully model MOC and enable functional drug testing. Trametinib exhibited antiproliferative effects in *KRAS*-mutated, MEK1/2-positive cell lines, suggesting MEK inhibition as a promising targeted approach for MOC.

Zusammenfassung

Hintergrund: Muzinöses Ovarialkarzinom (MOC) ist eine seltene Unterform des epithelialen Ovarialkarzinoms mit schlechter Prognose und limitierten Behandlungsmöglichkeiten. Die aktuelle Behandlungsstrategie ist basierend auf high-grade serösem Ovarialkarzinom und beinhaltet zytoreduktive Operationen und Platin-basierte Chemotherapie, welche in MOC schlechte Wirksamkeit zeigen.

Ziele: Es besteht eine Notwendigkeit passende präklinische Modelle und effektive, personalisierte Therapien zu entwickeln. Deshalb ist es das Ziel dieser Arbeit ein Model mit Zellkulturen von Patientengewebe zu etablieren, in welchem der MEK1/2 Inhibitor Trametinib in MOC getestet werden kann. Die Hypothesis lautet, dass Trametinib antiproliferative Effekte in Zelllinien mit MEK1/2 Expression zeigen soll.

Methoden: Zelllinien von Patienten und dazugehörige Organoide wurden etabliert, um die Ähnlichkeit zur Tumor Heterogenität und Architektur zu den ursprünglichen Tumoren zu zeigen. Trametinib wurde durch live-cell imaging, Viabilität- und Zytotoxizitätsassays getestet und mit dem Standardchemotherapeutikum Carboplatin verglichen. Weiters wurden Proliferation, Apoptose und Zielinhibierung mittels IHC-Färbung getestet.

Ergebnisse: Die Organoide zeigten morphologische und immunhistochemische Ähnlichkeit zu den originalen Tumorgeweben und bewiesen damit ihre Eignung für Medikamententests. Trametinib in einer Konzentration von 10 µM zeigte effektive Reduktion der Proliferation ohne Induktion von Apoptose, sichtbar bei der verminderten Ki67 Expression und der unveränderten cleaved caspase 3 Expression. Der Verlust des downstream Markers c-fos bestätigte die Inhibierung des MAPK-Signalwegs. Die Wirkungsintensität variierte zwischen den Zelllinien abhängig von ihrer MEK1/2 Expression und ihrem *KRAS*-Mutationsstatus.

Schlussfolgerung: Die Ergebnisse zeigten, dass von Patienten etablierte Organoid erfolgreich MOC replizieren und damit Medikamtententests ermöglichen. Trametinib zeigte antiproliferative Effekte in *KRAS*-mutierte, MEK1/2-positive Zelllinien, wodurch eine MEK-Inhibierung eine Möglichkeit zur Behandlung von MOC darstellt.

Table of Contents

List of abbreviations

Abbreviation	Full name
Arg	Arginine
Asp	Aspartic acid
BRAF	B-Raf Proto-Oncogene, Serine/Threonine Kinase
BRCA1	Breast Cancer Type 1
BRCA2	Breast Cancer Type 2
CA 125	Cancer Antigen 125
CA 19-9	Cancer Antigen 19-9
Casp3	Cleaved caspase3
CK20	Cytokeratin 20
CK7	Cytokeratin 7
CRC	colorectal cancer
DMSO	Dimethyl Sulfoxide
EGFR	Epidermal Growth Factor Receptor
EpCAM	Epithelial Cell Adhesion Molecule (CD326)
FBS	Fetal bovine serum
g	g-force
Gly	Glycine
HER2	Human Epidermal Growth Factor Receptor 2
His	Histidine
IHC	Immunohistochemistry
Ki-67	Kiel 67 – proliferation marker
KRAS	Kirsten Rat Sarcoma Viral Oncogene Homolog
MAPK	Mitogen-activated protein kinase
MEK1/2	Mitogen-Activated Protein Kinase Kinase 1/2
MOC	mucinous ovarian cancer
mTOR	Mechanistic target of Rapamycin
MUC1	Mucin 1
p53	Tumour protein 53
PCCL	Primary-derived primary cancer cell lines
PDO	Patient-derived organoid
PI3K	Phosphoinositide 3-kinase
RAS	Rat Sarcoma
RTqPCR	Reverse transcription quantitative polymerase chain reaction
STK11	Serine/Threonine Kinase 11
TP53	tumour protein 53
Trp	Tryptophan
Val	Valine
VEGF	Vascular Endothelial Growth Factor

1. Objectives

Mucinous ovarian cancer (MOC) is a rare subtype of ovarian cancer, and consequently, research on MOC remains limited. Due to its histological similarity to gastrointestinal tumours and derivation from high-grade serous ovarian cancer (HGSOC), MOC presents unique therapeutic challenges. Unlike HGSOC, there is currently no standard treatment regimen for MOC, and conventional platinum-based chemotherapy has shown limited effectiveness. Interestingly, MOC frequently exhibits high expression levels of MEK1/2 and *KRAS* mutations, suggesting that MEK inhibition could represent a promising personalized treatment strategy. This thesis aims to investigate the therapeutic potential of the MEK inhibitor Trametinib in mucinous ovarian cancer. Therefore, patient-derived cell lines are established and subjected to genetic analysis and clinical follow-up review. These cell lines will be further developed into three-dimensional organoid models that preserve the architecture and biomarker expression of the original tumour tissue. Drug testing will be performed using Trametinib, employing a combination of live-cell imaging, cell viability and cytotoxicity assays, and immunohistochemical staining in organoids to assess protein expression changes. This multi-level analysis enables a comprehensive evaluation of Trametinib's efficacy in MOC. Another key objective of this thesis is the establishment and characterization of organoid models derived from MOC patient samples. The organoids serve as a more physiologically relevant model system for drug testing and biomarker discovery, bridging the gap between traditional 2D cultures and *in vivo* tumours, and potentially facilitating the development of more effective, personalized therapies for MOC.

2. Introduction

2.1. Mucinous ovarian cancer (MOC)

MOC is one of the rare subtypes of ovarian cancer accounting for only 3% of all epithelial ovarian cancer (1). Patients typically undergo surgery for a suspicious pelvic mas before being diagnosed (2). MOC often presents as a large, unilateral, multicystic ovarian mass without prior peritoneal involvement. It evolves from benign mucinous cystadenomas to borderline mucinous tumours in a stepwise fashion until it develops into an invasive mucinous carcinoma (3). It is typically less likely to spread to the lymph nodes or upper abdomen compared to other ovarian cancer types (4).

Optimal debulking surgery to increase survival is the cornerstone of disease management (5). Adjuvant systemic therapy is recommended by the National Comprehensive Cancer Network guidelines in form of carboplatin-paclitaxel treatment, capecitabine-oxaliplatin treatment and leucovorin-5-FU-oxaliplatin treatment (2). The European Society of Medical Oncology recommend carboplatin-paclitaxel as the standard treatment, even though non-high-grade serous ovarian cancer have lower chemosensitivity. MOC is not mentioned specifically in the guideline (6). The lower chemosensitivity is shown as only 20 – 60 % of MOC patients respond to platinum-based chemotherapeutics (7). The resistance to standard platinum-based chemotherapeutics in advanced stages of MOC correlates with rapid disease progression and median survival of 12-14 months. Moreover, MOC shows low recurrence rates in early-stage disease, while advanced-stage leads to a dismal prognosis (8).

2.1.1. Histopathology and Genetics of MOC

Generally speaking, MOC shows more shared characteristics with gastrointestinal malignancies than with HGSOC, such as its molecular profile and clinical behaviour (9). Two subtypes of mucinous tumour can be found: the expansile and infiltrative subtype (10). The expansile subtype typically shows confluent glandular growth patterns, with minimal to no healthy ovarian stroma, while the infiltrative subtype produces malignant glands causing destructive stromal invasion (10, 11). Further, the expansile MOC has lower tumour spreading potential and risk of relapse. In contrast, the infiltrative MOC shows more aggressive

behaviour by forming more advanced, nonlocalized tumours and earlier tumour spreading (12, 13).

MOC seems to be driven by molecular alterations in the mitogen-activated protein kinase (MAPK) pathway (14). MOC is further characterized by common alterations, such as the Kirsten Rat Sarcoma Viral Oncogene Homolog (*KRAS*) mutation (40 – 65%), Human Epidermal Growth Factor Receptor 2 **(***HER2*) amplification and tumour protein p53 (*TP53*) mutation (15-17). Even though *TP53* mutations co-occur frequently with *KRAS* mutations in MOC, impairment of homologous recombination pathway (i.e. *BRCA* mutations) rarely happens (5). Moreover, 90% of MOC tumours are immunogenically "cold", meaning immunotherapy will likely not elicit a response (14-18).

2.1.2. Protein expression in MOC cells

Most mucinous ovarian cancer can be characterized by certain immunohistochemical markers, such as EpCAM, MUC1, CK7, CK20, CA 19-9, CA 125, HER2, MEK1/2 and CyclinE1.

EpCAM is a transmembrane glycoprotein and carcinoma-associated antigen, primarily expressed in epithelial tissues and various carcinomas, including gastrointestinal and ovarian cancers (19). In normal tissues, EpCAM is predominantly located in the intercellular spaces of epithelial cells, particularly in areas requiring tight cell-cell contact (20). Functionally, EpCAM plays a role in maintaining epithelial integrity by mediating homophilic cell-cell adhesion. It also contributes to proliferation and differentiation and is upregulated during inflammatory and regenerative processes (19, 20). In cancer, EpCAM shows intense, uniform overexpression on the cell membrane (21, 22). This overexpression can facilitate epithelial-mesenchymal transition (EMT) by decreasing E-cadherin expression, thereby promoting metastasis (23, 24).

MUC1 is a high-molecular-weight transmembrane glycoprotein and oncoprotein, commonly overexpressed in adenocarcinomas, including epithelial ovarian cancers (25). In normal tissues, MUC1 is expressed on the apical surface of glandular epithelial cells in the respiratory, gastrointestinal, and reproductive tracts (26). The protein functions in lubrication and protection of epithelial surfaces. In cancer, it also engages in intracellular signalling, affecting growth and proliferation via interactions with β-catenin and ErbB2 (27, 28). In epithelial ovarian cancer, MUC1 is overexpressed in over 90% of cases, including platinum-resistant tumours (29). This overexpression contributes to tumour progression, promotes metastasis

(30), and can mask cancer cells from immune surveillance (31). Knockout studies in transgenic mouse models show that loss of MUC1 delays tumour onset (32).

CK7 is a type II cytokeratin used as a diagnostic marker in pathology. It is widely expressed in glandular and transitional epithelia. In healthy tissues, CK7 is found in the cervical and endometrial glands, fallopian tubes, and epithelial cells of the placenta, but is absent in normal ovarian surface epithelium (33). In tumours, CK7 expression becomes non-specific and is seen in 59 out of 85 epithelial tumour types (33). In mucinous ovarian carcinomas (MOC), 92% of tumours are CK7-positive, indicating strong diagnostic relevance (33).

CK20 is another intermediate filament protein used in cancer diagnostics, with more restricted expression in normal tissues. It is typically expressed in the gastrointestinal tract and urothelium (33). In cancer, CK20 is upregulated in several tumour types, including mucinous ovarian, pancreatic, and urothelial carcinomas. Co-expression patterns of CK7 and CK20 are diagnostically valuable: colorectal adenocarcinomas are often CK20+/CK7− (34), while 63% of mucinous ovarian carcinomas express both CK20 and CK7 (35). In contrast, non-mucinous ovarian cancers typically show a CK20−/CK7+ profile (33).

CA 19-9 is a tumour-associated glycoprotein antigen used as a serum biomarker, especially in mucinous tumours. In cancer, serum CA 19-9 is often elevated in mucinous tumours of the pancreas, ovaries, biliary tract, and gastrointestinal system (36). The marker's level correlates with tumour size (37)(Kyung et al., 2009). In mucinous ovarian carcinomas, Cho *et. al.* found that 45.5% of malignant cases showed elevated CA 19-9 levels (38).

CA 125 is a high-molecular-weight glycoprotein and one of the most commonly used biomarkers for ovarian cancer. In normal tissues, CA 125 is produced by mesothelial cells of the peritoneum, pleura, and pericardium (39). Clinically, CA 125 is used to monitor disease progression in epithelial ovarian cancer (40). However, its diagnostic utility in mucinous ovarian tumours is limited: CA 125 levels often remain normal in these patients. Cho *et. al.* reported CA 125 elevation in only 27.3% of malignant mucinous ovarian tumours (38). Other studies have similarly shown limited elevation in primary MOC (41-43).

2.1.3. Protein expression of potential therapeutic targets

MEK1/2 are dual-specificity kinases that function as part of the MAPK/ERK signalling pathway. In normal tissues, MEK1/2 are expressed ubiquitously in proliferating cells (26). Their primary function is to phosphorylate ERK1/2, regulating cell growth, proliferation, differentiation, and survival (44). In cancer, MEK1/2 can become hyperactivated, often through upstream mutations (e.g., *KRAS*, *BRAF*), leading to enhanced proliferation and resistance to apoptosis. This makes MEK1/2 an attractive therapeutic target, particularly in tumours like MOC where MAPK signalling is frequently deregulated (44).

HER2 is a member of the EGFR family and a receptor tyrosine kinase involved in cell growth and survival. In normal tissues, HER2 is expressed at low levels in various epithelial cells (26). In mucinous ovarian carcinoma, HER2 overexpression is seen in a subset of cases—Han *et. al.* reported HER2 positivity in 26% of MOC tumours (45). However, clinical responses to HER2-targeted therapies, such as trastuzumab, have shown variable outcomes (46, 47).

Cyclin E1 is a regulatory protein involved in controlling the cell cycle. In normal tissues, Cyclin E1 is expressed during the late G1 phase to promote entry into the S phase (26). Functionally, Cyclin E1 forms a complex with CDK2 to drive G1/S phase transition and ensure proper DNA replication (48). In cancer, Cyclin E1 is frequently overexpressed due to cell cycle deregulation. This overexpression contributes to uncontrolled proliferation and may also be associated with chemoresistance (48).

2.1.4. Protein expression of drug testing related markers

Ki67 is a marker for cellular proliferation. It is expressed in the nucleus of cells that are actively dividing. This makes it a valuable tool for assessing cell proliferation in both physiological and pathological conditions (49). In healthy tissues, Ki67 is typically found in proliferative compartments such as the basal layers of stratified epithelia, including the skin and gastrointestinal tract (49). In cancer, elevated Ki67 levels are generally associated with a poorer prognosis, reflecting the tumour's high proliferative capacity (50).

Caspase 3 is a marker for apoptosis and the main mechanism for cell elimination of damaged cells (51). It acts as the executioner in the apoptotic pathway and needs to be activated via cleavage (52). The active enzyme degrade cellular proteins and causes DNA fragmentation (53). Its dysfunction leads to various diseases, most importantly cancer (54). This makes cleaved caspase 3 an interesting marker to observe apoptosis.

c-Fos acts as a transcription factor, downstream of MEK1/2 in the MAPK pathway and influences transcription. A study by Mahner *et. al.* found that higher c-fos expression is associated with longer recurrence-free periods and increased overall survival (55). Another study by Wang *et. al.* found that MEK inhibitors in turn downregulate c-fos and improve CAR-T treatments by preventing cell exhaustion (56).

2.2. Current treatment standard

Typically, patients undergo optimal debulking surgery, in which the tumor mass will be removed as much as possible (5). Due to the low incidence of MOC and the lack of effective chemotherapeutics, patients receive the same medication as serous ovarian cancer patients. The first-line adjuvant treatment commonly contains Carboplatin and Paclitaxel (9), to which MOC often shows a poor or absent response (4, 57). A retrospective study by Pectasides et. al. found that only 39% of MOC patients show a positive response to platinum-based chemotherapy compared to 70% in serous ovarian cancer (58). Due to the histological similarities between MOC and mucinous tumours in the gastrointestinal tract, MOC patients could benefit from gastrointestinal chemotherapy regimens, which includes 5-fluorouracil and oxaliplatin (59, 60).

2.2.1. Carboplatin

Carboplatin is a chemotherapeutical agent used in the treatment of advanced ovarian cancer and as part of palliative care for patients with the disease. Its structure is similar to that of cisplatin. Functionally, Carboplatin acts as an antineoplastic agent. It inhibits cancer cell proliferation by attaching alkyl groups to nucleotides, leading to the formation of monoadducts. These, in turn, cause DNA fragmentation—a form of DNA damage that leads to increased mutations, eventually triggering apoptosis due to cellular malfunction. Clinically, Carboplatin is administered intravenously in advanced ovarian cancer settings.

It is associated with fewer gastrointestinal and renal side effects than cisplatin, notably less nephrotoxicity and vomiting (61). In MOC, the response rates to standard platinum-based treatments are notably poor. In a retrospective series, only ~35 % of MOC patients had a partial response to first-line carboplatin-paclitaxel combination treatment (4, 57, 58, 62).

2.2.2. Paclitaxel

Paclitaxel is a chemotherapeutical agent classified as a tetracyclic diterpenoid, originally isolated from the Pacific yew tree *Taxus brevifolia*. As an antineoplastic drug, Paclitaxel works by stabilizing microtubules, thereby preventing their disassembly. This stabilization causes the microtubules to cluster into bundles, disrupting the dynamic reorganization of the microtubule network that is necessary for mitosis. Consequently, cell division is halted, and cellular proliferation is inhibited. Paclitaxel is used in the treatment of epithelial ovarian cancer, Kaposi's sarcoma, breast cancer, non-small cell lung cancer, peritoneal cancer, and fallopian tube cancer. Reported side effects include developmental and reproductive toxicity, which occurs regardless of biological sex (63). Paclitaxel shows a poor response in MOC, as mentioned above (4, 57, 58, 62).

2.2.3. Bevacizumab

Bevacizumab is a monoclonal antibody that functions as a chemotherapeutical agent through the inhibition of vascular endothelial growth factor (VEGF). VEGF plays a critical role in cell survival and proliferation. Bevacizumab works by binding to the VEGF receptor, restoring a more normalized vasculature in the tumour environment. This not only inhibits metastasis but also improves the delivery of co-administered chemotherapeutic agents. It is used in several types of cancer, including epithelial ovarian cancer, colorectal cancer (CRC), fallopian tube cancer, breast cancer, renal cancer, non-squamous non-small cell lung cancer, and glioblastoma. In advanced epithelial ovarian cancer, it is commonly used in combination with Carboplatin and Paclitaxel. The drug is administered intravenously or intramuscularly, as it would be degraded in the stomach if taken orally (64). The report from Tarumi *et. al.* showed favourable outcomes in the patient and Winer *et. al.* showed prolonged response in their patient (65, 66). However, no larger studies outside of case reports have been published yet.

2.2.4. Doxorubicin Hydrochloride

Doxorubicin Hydrochloride, commercially known as caelyx, is an antineoplastic agent used primarily in cases of advanced ovarian cancer, particularly when first-line platinum-based chemotherapy has failed. Mechanistically, the drug inhibits topoisomerase II, an enzyme essential for relaxing the supercoiled DNA ahead of the replication fork during DNA synthesis. Inhibiting this enzyme results in DNA fragmentation, which leads to increased mutations and eventual apoptosis of the affected cells due to loss of genomic integrity (67). Pignata *et. al.*, as well as Pisano *et. al.* found no response to doxorubicin in MOC in their studies (62, 68).

2.3. MAPK pathway

The MAPK pathway is a key pathway, which regulates cell proliferation, cell differentiation and cell death. It is activated by extracellular mitogens, like the epidermal growth factor (EGF). EGF binds to its receptor tyrosine kinase (EGFR) and induces autophosphorylation, see figure 1. This recruits the adaptor protein GRB2 and SOS, which leads to a subsequent GDP-GTP exchange on RAS (69). KRAS mutations constantly keep RAS in a GTP-bound and active state. The activated KRAS recruits RAF kinases, such as BRAF. BRAF in turn phosphorylates MEK1/2. The activated MEK1/2 phosphorylates ERK1/2 for activation. ERK translocates into the nucleus to activate transcription factors like ELK1 and c-MYC via phosphorylation. The activated transcription factors regulate genes that causes proliferation, differentiation and apoptosis (70, 71).

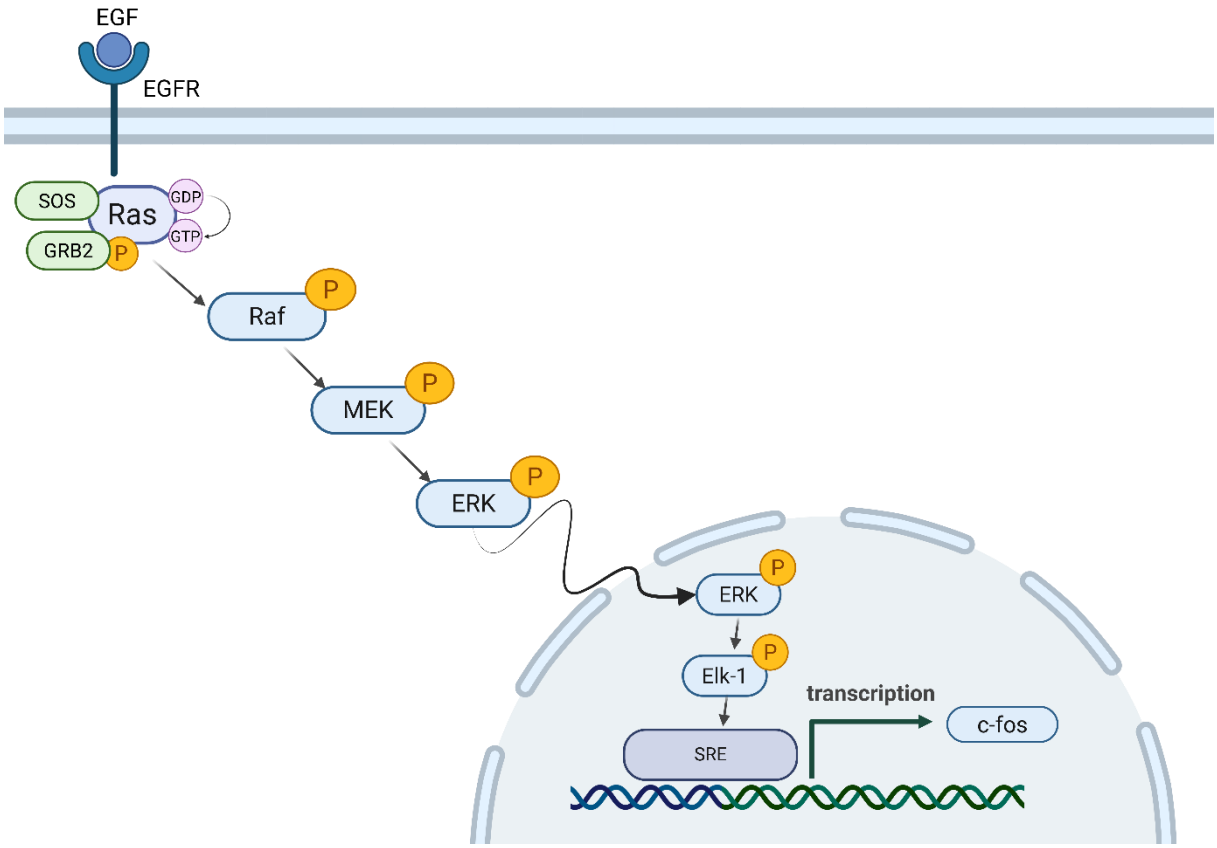

Figure 1: MAPK pathway, created with BioRender.com.

2.4. Targeting the MAPK pathway via MEK inhibition

Because the MAPK pathway is commonly activated in mucinous ovarian cancer (MOC), especially due to frequent KRAS mutations, targeting this pathway is an attractive therapeutic strategy. A number of preclinical studies have shown synergy between inhibition of MEK (Mitogen-Activated Protein Kinase Kinase) and PI3K in MOC cell lines harbouring KRAS mutations (72). MEK inhibitors are a class of targeted therapy agents that selectively inhibit MEK1 and MEK2, which are key kinases in the RAS-RAF-MEK-ERK signalling cascade. These inhibitors bind to a pocket adjacent to the ATP-binding site and stabilize MEK in an inactive conformation. This prevents MEK from phosphorylating ERK, thus interrupting downstream signalling (73). Trametinib is a MEK1/2 inhibitor and antineoplastic agent (74). Before Trametinib, other MEK inhibitors were limited by toxicity concerns in non-malignant cells, which also depend heavily on MAPK pathway signalling (75). Trametinib overcomes part of the narrow therapeutic index of MEK inhibition because of its prolonged half-life and small peak-to-trough ratio (76). In vitro and preclinical studies demonstrate efficacy of Trametinib: for example, the SelleckChem data in the HT-29 colorectal cancer cell line shows good efficacy

(76, 77). In experiments by Solit et al., BRAF-mutated cell lines showed a more marked response to Trametinib; RAS-mutated cell lines responded only partially (78). Predictive biomarkers for sensitivity to Trametinib include mutations in RAF, RAS, PIK3CA/PTEN, and DUSP6 (44, 45). Mechanistically, Trametinib reduces cell proliferation, induces cell cycle arrest in G1 phase, and can lead to senescence (45). Although preclinical ovarian cancer cell line studies have shown efficacy of Trametinib, none of them used mucinous ovarian cancer (MOC) cell lines (79). Regarding pharmacokinetics and toxicity: Trametinib is orally bioavailable (74). It causes increases in serum aminotransferase and alkaline phosphatase. It is degraded by deacetylation via carboxylesterase and eliminated in both feces and urine (74). In a broad screen of cancer cell lines (in vitro), about 76% of tested lines exhibited either cytotoxic or cytostatic responses to Trametinib (80). Schubbert et al. noted that KRAS mutations (in cancers of the colon, lung, pancreas, and cervix) confer sensitivity to Trametinib (81). Clinical trials have also reported several side effects of Trametinib, including dermatitis acneiform, diarrhoea, rashes, and central serous retinopathy (82).

2.5. Experimental model systems

There are currently approximately 100 publicly available ovarian cancer cell lines, but only a few are MOC cell lines (83). Therefore, the establishment of patient-derived cell lines is important, as they show the diversity found in patients (84). Primary-derived primary cancer cell lines (PCCL) are established by taking patient tumour tissue and enzymatically, chemically or mechanical digesting it before placing it in culture medium to grow, after minimal passaging, cell lines can be establish (85).

Cell line models are *in vitro* cultures of immortalized cancer cells widely used in cancer research (86). These cells are established by isolating tumour tissue, enzymatically dissociating it, and propagating the cells under controlled conditions (86). They are extensively used in preclinical research for high-throughput drug screening, molecular biology studies, and mechanistic investigations (87). Cell lines are cost-effective, easy to handle, and reproducible (86). However, they often lack the tumour microenvironment and genomic heterogeneity found in primary tumours, which limits translational relevance (86). Additionally, long-term passaging may lead to genotypic and phenotypic drift (87). Genomic profiling studies have further highlighted these limitations. Domcke *et. al.* performed a comprehensive comparison of 47 commercially available ovarian cancer cell lines. Their analysis revealed that many

commonly used ovarian cancer cell lines, such as SK-OV-3, show substantial genomic divergence from HGSOC, often lacking key alterations such as *TP53* mutations or exhibiting mutation patterns characteristic of other subtypes. In contrast, only a small subset of lines—including KURAMOCHI, OVSAHO, OVCAR-4, COV362, and COV318—closely recapitulated the genomic and transcriptomic landscape of HGSOC. These findings underscore the importance of molecularly informed model selection and highlight the need to establish and characterize ovarian cancer cell lines that faithfully represent the major clinical subtypes (88).

Patient-derived xenograft (PDX) models are created by implanting fresh human tumour tissue into immune-deficient mice. The tissue is typically obtained from surgical resection or biopsy and engrafted subcutaneously or orthotopically. These models are used in translational cancer research to evaluate drug efficacy, study tumour heterogeneity, and model resistance mechanisms. PDX models retain the histological and genetic features of the original patient tumour (89). While they better reflect human cancer biology than cell lines, they are time-consuming, costly, and require immunocompromised hosts, limiting immune-oncology studies (90). In ovarian cancer research, Cybulska *et. al.* established and genomically characterized a large collection of HGSOC PDX models, demonstrating that these recapitulate the genetic, histological and pharmacological features of patient tumours. The PDXs preserved hallmark HGSOC alterations such as near-universal *TP53* mutations, frequent *BRCA1/2* mutations and characteristic copy number variations, closely mirroring the cancer genome atlas data. The xenografts reproduced patient-specific responses to platinum-based chemotherapy, accurately reflecting clinical sensitivity or resistance (91).

Organoids and spheroids are three-dimensional (3D) culture models derived from stem cells or primary tumour cells. They are established by embedding cells in a supportive matrix like Matrigel and culturing them with specific growth factors to promote self-organization (92). Organoids mimic the architecture, heterogeneity, and function of original tissues, while spheroids, formed from aggregated cells, offer simpler 3D structures (92, 93). These models are increasingly used in personalized medicine, drug screening, and studying tumour biology *in vitro* (92). Although they offer higher physiological relevance than 2D models, limitations include complex setup, lack of vasculature, and challenges in modelling immune components (92, 93). In ovarian cancer research, Graham *et. al.* established a reliable and reproducible protocol for generating patient-derived organoids (PDOs) from HGSOC tissue, ascites and pleural fluid. These organoids preserved the histological, cytological and genetic features of their parental tumours. They can maintain long-term viability even through serial passaging

and cryopreservation. Further, they retained key aspects of tumour heterogeneity, providing a physiologically relevant *in vitro* model for studying ovarian cancer, its drug sensitivity and resistance mechanisms. Despite the gradual loss of immune cells with continued culture, the study demonstrated that HGSOC PDOs represent a robust platform for translational research and personalized therapeutic testing (94). The study by Nanki *et. al.* demonstrated that organoids can be grown from single cells into organoids with the help of Matrigel and still recapitulate a gene and protein expression similar to the original tumour tissue, as the organoids did not acquire major novel chromosomal aberrations (95).

3. Methods

3.1. Clinical materials

The cell lines TG024, TG050 and 8867 were established from tumour tissue of patients with mucinous ovarian cancer (MOC), while the cell line TG089 was established from the ascites of a MOC patient. Tumour tissues or ascites were obtained from the Department of Obstetrics and Gynecology and their histopathological characteristics were assessed by two independent pathologists from the Department of Pathology, Medical University of Vienna. The clinical specimens were transferred to the laboratory for further processing. The cell line HT-29 was provided by Priv.-Doz. Mag. pharm. Martin Schepelmann, PhD. All procedures were approved by the local ethic committee (EK Nr. 366/2003 and 260/2003) and informed consents have been obtained from all patients.

3.2. Establishment of cell lines and organoids

To establish cell lines from tumour tissue, it was scraped with a cell scraper into PBS. The cell suspension was then filtered through a 40 µm nylon cell strainer (Falcon, Corning® Incorporated, Corning, NY, USA). The cell strainer was inverted and washed with PBS to collect the cell clusters, followed by a final wash with medium – DMEM/F-12 (1:1) (1X) + GlutaMax-I (Gibco, Life Technologies Limited, Paisley, UK) supplemented with 10% Fetal Bovine Serum (FBS), 100 Units/ml Penicillin and 100 µg/ml Streptomycin (Gibco, Life Technologies Limited). The cells were seeded into 25 cm² Nunc EasyFlask (Nunc A/S, Thermo Fisher Scientific, Roskilde, Denmark). Cell cultures were maintained at standard conditions – 37 °C in 5% CO2 atmosphere. Ascites samples were filtered directly through a 40 µl cell strainer and processed identically as for tumour tissues. Non-tumour cells from the initial cultures were depleted through repeated selective 2-minute trypsinization using 0.05% Trypsin-EDTA (1X) (Gibco, Life Technologies Limited).

For organoid establishment from cell lines, 5 x 10^5 cells were suspended in medium. The cell suspension was mixed in a 1:3 ratio with Matrigel (Corning Matrigel Matrix, Corning® Incorparted) on ice. The mixture was plated centrally in the well of a 24-well plate (Nunc A/S, Thermo Fisher Scientific). After incubation at 37 °C for 1 min for partial gelation, plated were inverted and further incubated for another 15 min. Afterwards organoids were maintained in the medium as described above.

3.3. Mutation detection of the *TP53*, *KRAS*, and *BRCA1/2* genes

Mutations in *TP53*, *KRAS*, and *BRCA1/2* were reassessed or confirmed from tissue of recurrent disease at the time of cell line establishment using the Ion AmpliSeq™ Cancer Hotspot Panel v2 (Thermo Fisher Scientific, Cat. No. 4475346). *BRCA* mutational status was assessed as part of clinical routine. Starting in 2020, tumour tissue was routinely subjected to homologous recombination deficiency (HRD) testing, using the Myriad myChoiceR CDx PLUS assay (Myriad Genetic Laboratories, Salt Lake City, UT, USA).

3.4. Live-imaging for growth rate estimation and the determination of effective drug concentrations

The IncuCyte SX3 live-cell analysis system (Satorius AG, Göttingen, Germany) was used to estimate the growth rate of each cell line. Cells were seeded in 96-well Clear Flat Bottom plates (Corning® Incorporated) at an initial density of 20 % and maintained at standard conditions for varying periods. Images were captured at 10X every six hours over the incubation period, with five images captured per well. The average confluence percentage was plotted against the time in hours and the doubling time was estimated from the growth curve.

For drug testing, cells were seeded with an initial density of ~20 % per well in 200 µl medium and incubated at standard conditions overnight. Medium, 150µM Carboplatin (Accord Healthcare B.V., Utrecht, Netherlands), 1:200 DMSO (Merck KGaA, Sigma-Aldrich, Darmstadt, Germany) and 1:1000 DMSO were included in the test of each cell lines. Carboplatin, the standard treatment, was used as a reference. DMSO (the vehicle for Trametinib) was used as a control to exclude any solvent-specific effects. The cells were treated with 0.4 µM, 2 µM, 10 µM and 50 µM Trametinib (Selleck Chemicals LLC, Houston, TX, USA). The stock solution was dissolved in DMSO (Merck KGaA, Sigma-Aldrich), while the different concentrations were achieved by dilution in medium. Imaging conditions remained the same as above and phase confluence percentage was plotted against time.

3.5. Formalin-fixation paraffin embedding (FFPE) of organoid samples

Organoids were fixed in 4% paraformaldehyde in PBS for one hour and washed twice with PBS. Then, they were overlaid with 70% ethanol overnight at 4 °C. The organoids were incubated with 70 % ethanol containing 1 % alcian-blue solution at room temperature for 30 min. Specimens underwent sequential dehydration steps: two times 96 % ethanol for 10 min, two times 100 % ethanol for 15 min and two times xylene for 20 min. Samples were incubated in liquid paraffin for 30 min, followed by replacement with fresh paraffin. After solidifying of paraffin on a cooling plate for approximately 60 min, they were deposited at room temperature.

3.5.1. Sectioning of the FFPE blocks

FFPE tumour tissues from the operation were obtained from the Department of Pathology. FFPE blocks were sectioned at 4.5 µm thickness using a microtome (HM 355 S, Thermo Fisher Scientific). Sections were mounted on Superforst™Plus Adhesion Microscope Slides (Epredia, Breda, Netherlands), air-dried for 48 hours at room temperature and stored at -20 °C.

3.6. Immunohistochemistry staining

To perform immunohistochemistry, the slides were first incubated at 58 °C for 15 min and subsequently deparaffinised in Xylene twice for 5 min. For rehydration, sections were passed through descending concentrations of ethanol (100%, 96%, 80%, 70%), incubating for 3 min in each solution. The slides were washed in distilled water for 5 min and permeabilized with 0.5 % Triton in PBS for 15 min. The sections were washed twice in PBS for 3 min and once in distilled water for 2 min. For antigen retrieval (see table 1), the slides were incubated in citrate (pH 6.0) or Tris-EDTA (pH 9.0) buffer and microwaved at 850 watts, followed by 11 min at 160 watts. After microwaving, the slides were allowed to cool to room temperature. The sections were washed with distilled water for 5 min and a hydrophobic barrier was created. The tissue sections treated with 3 % hydrogen peroxide in methanol for 10 min. Non-specific binding was blocked using the ZytoChemPlus(HRP)Polymer Kit blocking solution (Zytomed Systems, Berlin, Germany) for 10 min. Another washing step was performed in PBS-Tween, twice for 3 min each. The primary antibodies were diluted in antibody diluent (Dako, Agilent, Glostrup, Denmark) according to table 1. The sections were incubated with the primary antibody overnight at 4 °C.

Table 1: Detailed information on the antibodies used for immunohistochemistry.

Antibody	Dilution	Company	Catalog number	Antigen retrieval
EpCAM	1:500	Abcam	ab32392	Citrate buffer
CA 19-9	1:300	Abcam	ab3982	Citrate buffer
CA 125	1:200	Leica Biosystems	NCL-L-CA 125	Citrate buffer
CK7	1:500	ThermoFisher Scientific	MA5-11986	Citrate buffer
CK20	1:100	ThermoFisher Scientific	MA5-13263	Citrate buffer
MUC1	1:750	NeoMarkers	MS-153PO	Citrate buffer
HER2	1:500	Dako	A0485	Citrate buffer
MEK1/2	1:500	Abcam	ab178876	Tris-EDTA buffer
Cyclin E1	1:1000	Abcam	ab71535	Citrate buffer
Cleaved CASP3	1:400	Cell Signaling	9661S	Citrate buffer
Ki-67	1:100	Dako	M7240	Citrate buffer
c-fos	1:500	Abcam	ab302667	Citrate buffer

The slides were then washed twice in PBS-Tween for 5 min and incubated with the secondary antibody solution (Reagent 2 from the ZytoChemPlus (HRP) Polymer Kit) for 20 min. The washing step was repeated followed by incubation with the chromogen solution (Reagent 3 from the ZytoChemPlus (HRP) Polymer Kit) for 30 min. For visualization, a substrate solution consisting of 1 mL substrate buffer mixed with 1 drop of DAB chromogen was applied (150 µL per slide) and developed for 2‑15 min, with the development time adjusted based on color intensity. The reaction was stopped with distilled water. The slides were counterstained in hematoxylin (Merck KGaA, Sigma-Aldrich) for 2 seconds and then washed with running tap water for 20 min. The slides were mounted with Kaisers Glycerolgelatine (Merck KGaA, Sigma-Adrich).

3.7. Cell viability and cytotoxicity assessment

To determine the relative number of living and dead cells, viability and cytotoxicity assays were performed using the CellTiter-Fluor™ Cell Viability Assay (G6082, Promega Corporation, Madison, WI, USA) and CellTox™ Green Cytotoxicity Assay (G873B, Promega Corporation). Experiments were conducted in 384-well black-walled clear-bottom plates (Corning Incorporated, Kennebunk, ME, USA), with each well containing a total volume of 40 µL comprising equal parts cell suspension (20 µL) and 2X treatment solution (20 µL). All assays were performed in clear/white DMEM/F-12 medium (21041-025, Gibco, Life Technologies Limited). Cells were maintained under standard conditions during the experiment. Cell line specific parameters were established as follows: TG024, TG050 and 8867 cell lines were seeded at 2000 cells per well. Measurements were performed every 48 hours for TG024 and 8867, while TG050 was measured every 72 hours. TG089 and HT-29 were seeded at 1000 cells per well and assessed every 24 hours due to higher proliferation rates.

The initial cell viability upon seeding was measured with the cell counter (Luna II, BioCat GmbH, Heidelberg, Germany) and used as the baseline. To measure the viability the cells were mixed with 4µl of GF-AFC substrate (1:1000) (G608B, Promega Corporation) on a thermomixer (Eppendorf Corporate, Hamburg, Germany) for 30 s at 700 min^{-1} with and then incubated for 30 min at 37°C. The fluorescence intensity was measured with the CLARIOstar Plus microplate reader (BMG LABTECH GmbH, Ortenberg, Germany) at a wavelength of 380/505 nm to show the relative viability in relation to the baseline measurement. Then, the cells were mixed with the CellTox Green Dye (G873B, Promega) on a thermomixer (Eppendorf Corporate) for 30s at 700 min^{-1} and incubated for 10 min at room temperature and again measured with the CLARIOstar Plus microplate reader (BMG LABTECH GmbH) at a wavelength of 485/520 nm.

3.8. Drug testing in organoids

Carboplatin (150 µM) and Trametinib (10 µM) were applied to organoids after 5 days of initial cultivation. Following drug exposure at 24 h and 72 h, organoids were processed to FFPE blocks using the method explained under section 1.5. For staining of proliferation, apoptosis and drug-related markers see section 1.6.

4. Results

4.1. High prevalent expression of MEK1/2 in MOC

The following IHC stainings were performed by a previous student (Anita Alberts) and were the basis for this project. MEK1/2 positivity was observed in all 24 MOC tumour tissues, irrespective of their expansile or infiltrative histopathological type (figure 2). These findings led to the hypothesis that inhibition of MEK could be a useful therapeutic strategy in mucinous ovarian cancer.

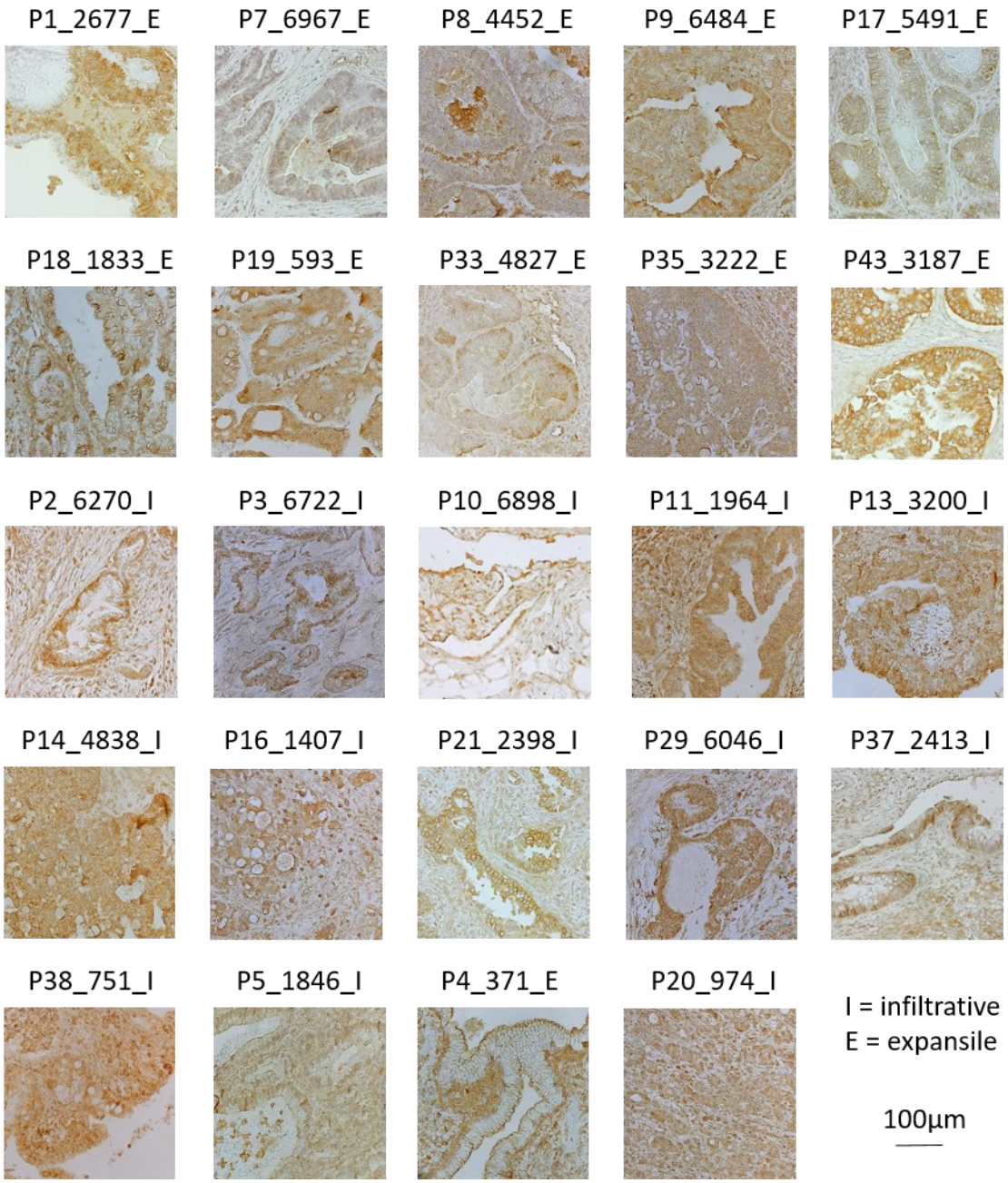

Figure 2: MEK1/2 staining of mucinous ovarian cancer tissue, created with stained samples from Anita Alberts.

4.2. Clinical and follow-up information of patients

Within this study four patient-derived cell lines – TG024, TG050, TG089 and 8867 – were used, as well as one commercially available control cell line – HT-29. The clinical treatment and disease progression of the four patients has been tracked, see figure 3. Due to data protection all names and personal information are anonymous and the patients, as well as the corresponding cell lines were coded. Patient 37 was diagnosed with MOC 48 days before debulking surgery. Cell line TG024 was established from tumor tissues obtained by surgery. The patient was treated with a combination of Carboplatin and Paclitaxel from day 45 to day 90. Cancer-related death occurred 163 days after debulking surgery.

Patient 39 was diagnosed with MOC 60 days before debulking surgery. TG050 were established from tumour materials taken 23 days before the surgery and on the day of surgery. The patient was treated with a combination of Carboplatin, Paclitaxel and Avastin from day 20 to day 131. The patient died of cancer about 4 months after the chemotherapy.

Patient 44 was diagnosed with MOC 28 days before debulking surgery. The patient was treated with a combination of Carboplatin and Taxol from day 195 to day 216. Cell line TG089 was established from ascites. Patient died 228 days after debulking surgery.

Patient 30 was diagnosed with MOC 7 days before their debulking surgery. A tumour sample was taken during debulking surgery to create the cell line 8867. The patient was treated with a combination of Carboplatin, Taxol and Avastin from day 22 to day 139. Then, a combinatorial treatment with Caelyx and Avastin followed from day 348 until day 447. Cancer-related death occurred 1403 days after debulking surgery.

The commercial colorectal cancer cell line HT-29 does not provide the patients history like the patient-derived cell lines, but the COSMIC database (96) provides information about relevant mutations.

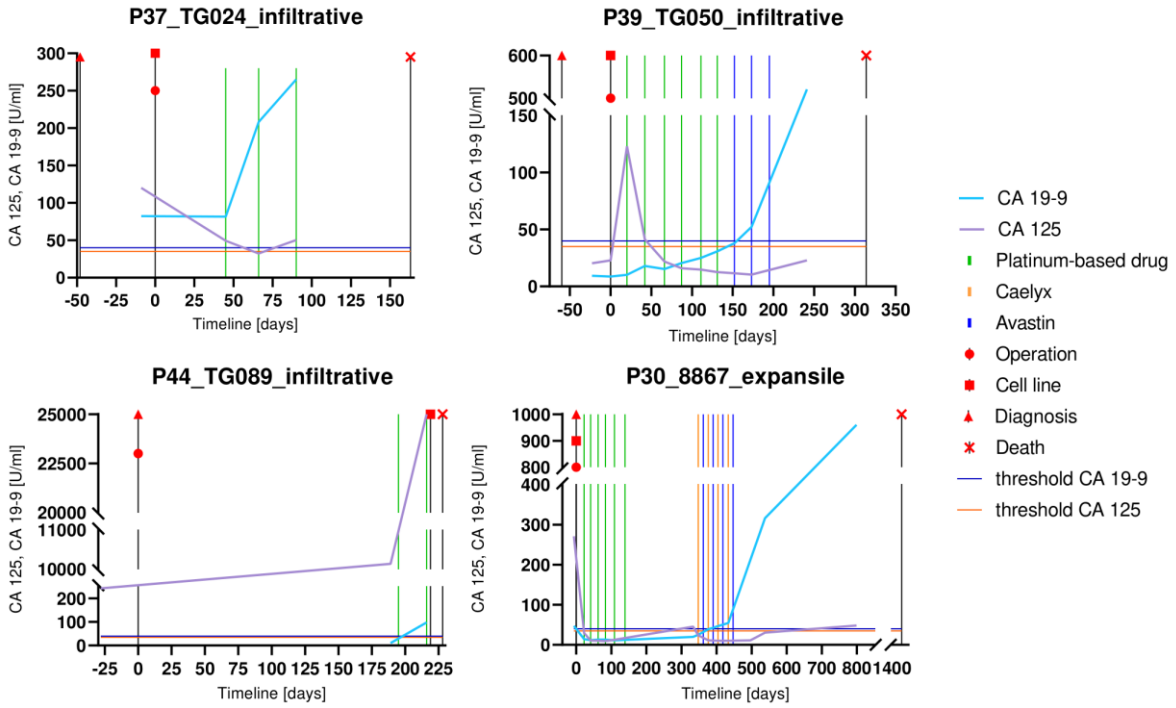

Figure 3: Clinical information, treatments and disease progression of the MOC patients. The day of debulking surgery is defined as day 0. The days of diagnosis, cell line establishment and death were indicated. CA19-9 and CA125 were assessed to monitor the disease progression. Each cycle of the treatments was show with a horizontal line. The corresponding organoids coding and their histopathologic types were also indicated.

4.3. Characteristics of the cell lines

The morphology of MOC cell lines is shown in figure 4. TG024, TG050 and TG089 are infiltrative mucinous ovarian tumours, while 8867 is an expansile MOC and HT-29 is a colorectal tumour. The cell lines showed different morphology in 2D culture. TG024 and TG050 showed polygonal shape, while TG089, 8867 and HT-29 are round. 8867 and HT-29 had an average cell size of 7 µm. TG024 and TG089 had an average cell size of 9 µm, while TG050 was bigger with an average cell size of 20 µm. TG089 and HT-29 doubled approximately every day, while TG024 and 8867 double every two days. TG050 had a doubling time of 75 hours (table 2).

The cell line TG024 showed mutations in the genes *TP53* and *KRAS* (table 3). *TP53* was a frameshift mutation at codon 863 that led to a transcription stop, while *KRAS* was a missense mutation, leading to the change of an amino acid glycine to aspartic at codon 35. The cell line TG050 showed mutations in the genes *TP53* and *KRAS*. *TP53* had a missense mutation, leading to the expression of tryptophan instead of arginine at codon 799. *KRAS* harboured a missense mutation, leading to the expression of aspartic acid instead of glycine at codon 35. The cell

line TG089 showed mutations in the genes *TP53* and *STK11*. *TP53* was a heterozygous missense mutation, leading to the expression of aspartic acid instead of glycine at codon 637, but also a nonsense mutation at codon 734 leading to a stop in translation. *STK11* was a nonsense mutation at codon 475, leading to the integration of a stop codon. The cell line 8867 showed mutations in the gene *KRAS*. *KRAS* was a missense mutation, leading to the expression of valine instead of glycine at codon 35. HT-29 had a homozygous *TP53* missense mutation at codon 818, where a histidine is expressed instead of an arginine.

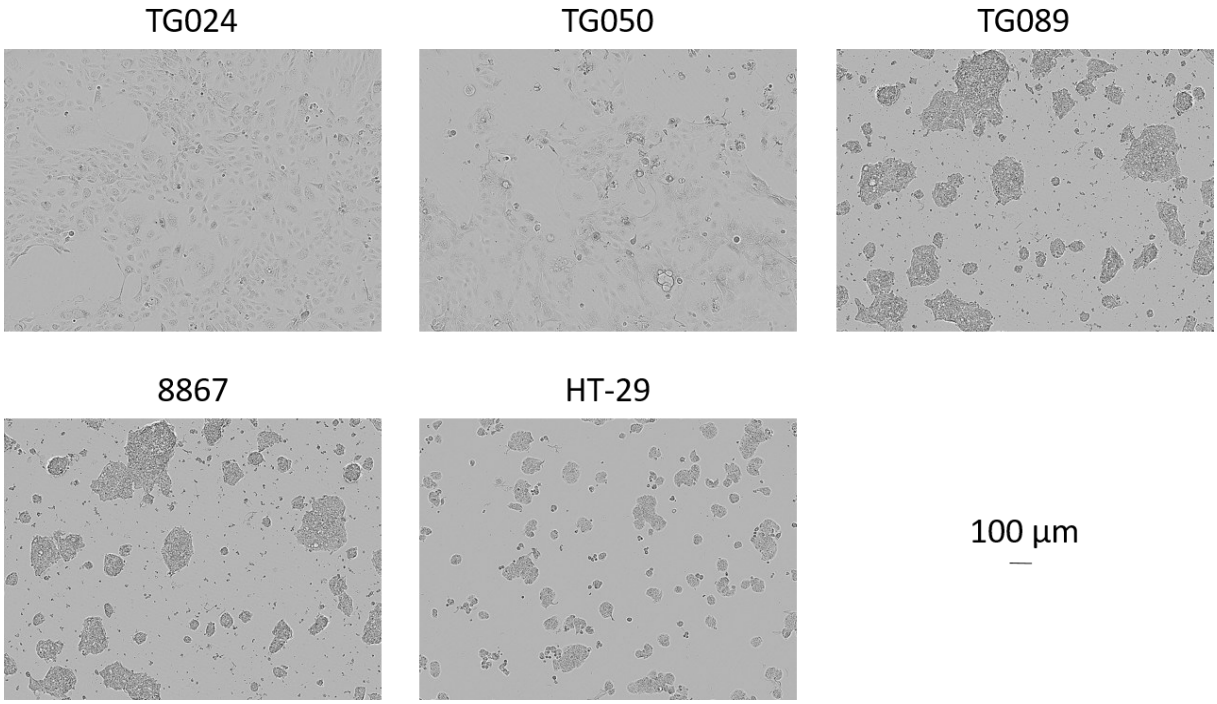

Figure 4: Morphology of the cell lines TG024, TG050, TG089, 8867 and HT-29. Captured by IncuCyte SX3 live-cell analysis system. Scale bar: 100 µm.

Table 2: Characteristics of MOC and CRC cell lines.

Cell line	**Histopathologic type**	**Size**	**Shape**	**Doubling time**
8867	Expansile	7 µm	round	2 days
TG024	Infiltrative	9 µm	polygonal	2 days
TG050	Infiltrative	20 µm	polygonal	3 days
TG089	Infiltrative	9 µm	round	1 day
HT29	Colorectal cancer	7 µm	round	1 day

Table 3: Overview of the mutations in the MOC and CRC cell lines.

Cell line	Patient number	Original material*1	Histopathology *2	*TP53* mutation*3	*TP53* mutation details	*BRCA1* mutation *3	*BRCA2* mutation *3	*KRAS* mutation *3	*KRAS* mutation details	*STK11* mutation *3	*STK11* mutation Details
8867	30	T	E	0	/	0	0	1	c.35G>T; p.Gly12Val	0	/
TG024	37	T	I	1	c.863del; p.Asn288Ilefs*57	0	0	1	c.35G>A; p.Gly12Asp	0	/
TG050	39	T	I	1	c.799C>T; p.Arg26Trp	0	0	1	c.35G>A; p.Gly12Asp	0	/
TG089	44	A	I	2	c.637C>T; p.Gyl245Asp c.734G>A; p.Arg213*	0	0	0	/	1	c.475C>T; Gln159*
HT29	/	T	CRC	1	c.818G>A; p.Arg273His	0	0	0	/	0	/

**1: Original material: T: tumour tissue; A: ascites; *2: Type of cancer: I: infiltrative; E: expansile; CRC: colorectal cancer; *3: mutations in tumour cells: 0: wild type; 1: homozygous; 2: heterozygous. Information about HT-29 mutations was taken from the COSMIC database (96)*.

4.4. Organoids from patient-derived cell lines recapitulate the original tumours

4.4.1. Organoids showed similar expression pattern and intensity of tumour related markers

In figure 5, EpCAM was positively expressed on the membrane of all organoid**s** (TG024, TG050, TG089, and 8867) and their corresponding tumour tissues. MUC1 was positively expressed on the cell membrane of all organoid cells and their corresponding tumour tissues except that the tumour tissues for TG024 and 8867 only showed partial MUC1 expression. All organoids recapitulated the EpCAM expression pattern of their parent tumours. A congruent expression pattern for MUC1 was also observed between organoids and tumour tissues for TG050 and TG089. In contrast, TG024 and 8867 organoids exhibited a divergent MUC1 expression pattern compared to their partially expressing tumour tissues.

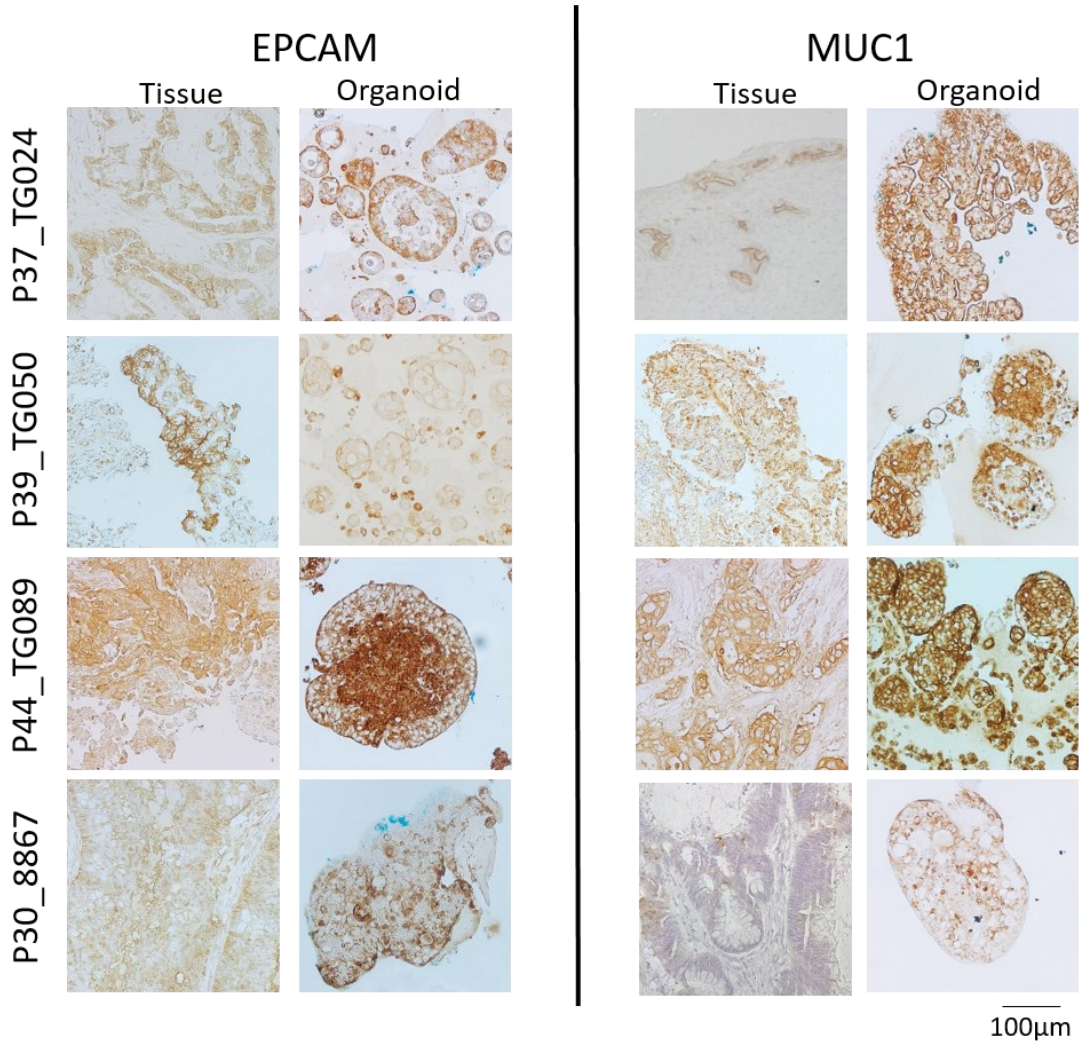

Figure 5: EPCAM and MUC1 expression by IHC in patient-derived organoids and their corresponding tumour tissues.

In figure 6, CK7 was positively expressed on the membrane of 3 organoid**s** (TG024, TG050 and TG089) and their corresponding tumour tissues. However, TG024 and TG050 expressed CK7 only partially. CK20 was partially positively expressed on the cell membrane of TG050 and 8867 organoid cells and their corresponding tumour tissues. All organoids recapitulated the CK7 expression pattern of their parent tumours. A congruent expression pattern for CK20 was also observed between organoids and tumour tissues for all organoids and their parent tumours.

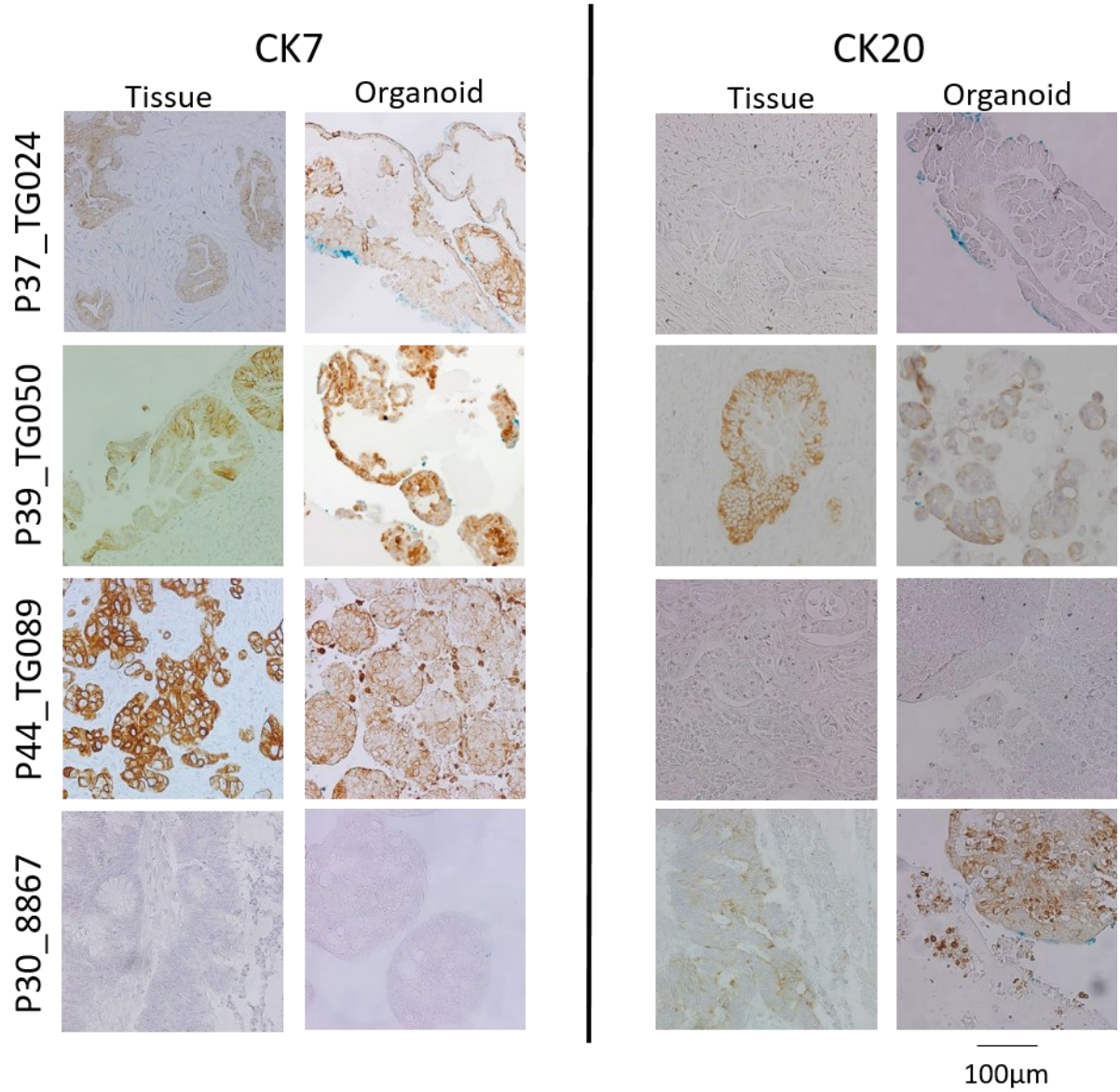

Figure 6: CK7 and CK20 expression by IHC in patient-derived organoids and their corresponding tumour tissues.

In figure 7, CA 19-9 was positively expressed on the membrane of all organoid**s** and their corresponding tumour tissues. However, TG089 and 8867 expressed CA 19-9 only partially. CA 125 was positively expressed on the cell membrane of TG024, TG050 and TG089 organoid cells and their corresponding tumour tissues, except that TG024 and TG050 only showed partial CA 125 expression. All organoids recapitulated the CA 19-9 expression pattern of their parent tumours. A congruent expression pattern for CA 125 was also observed between organoids and tumour tissues for all organoids and their parent tumours.

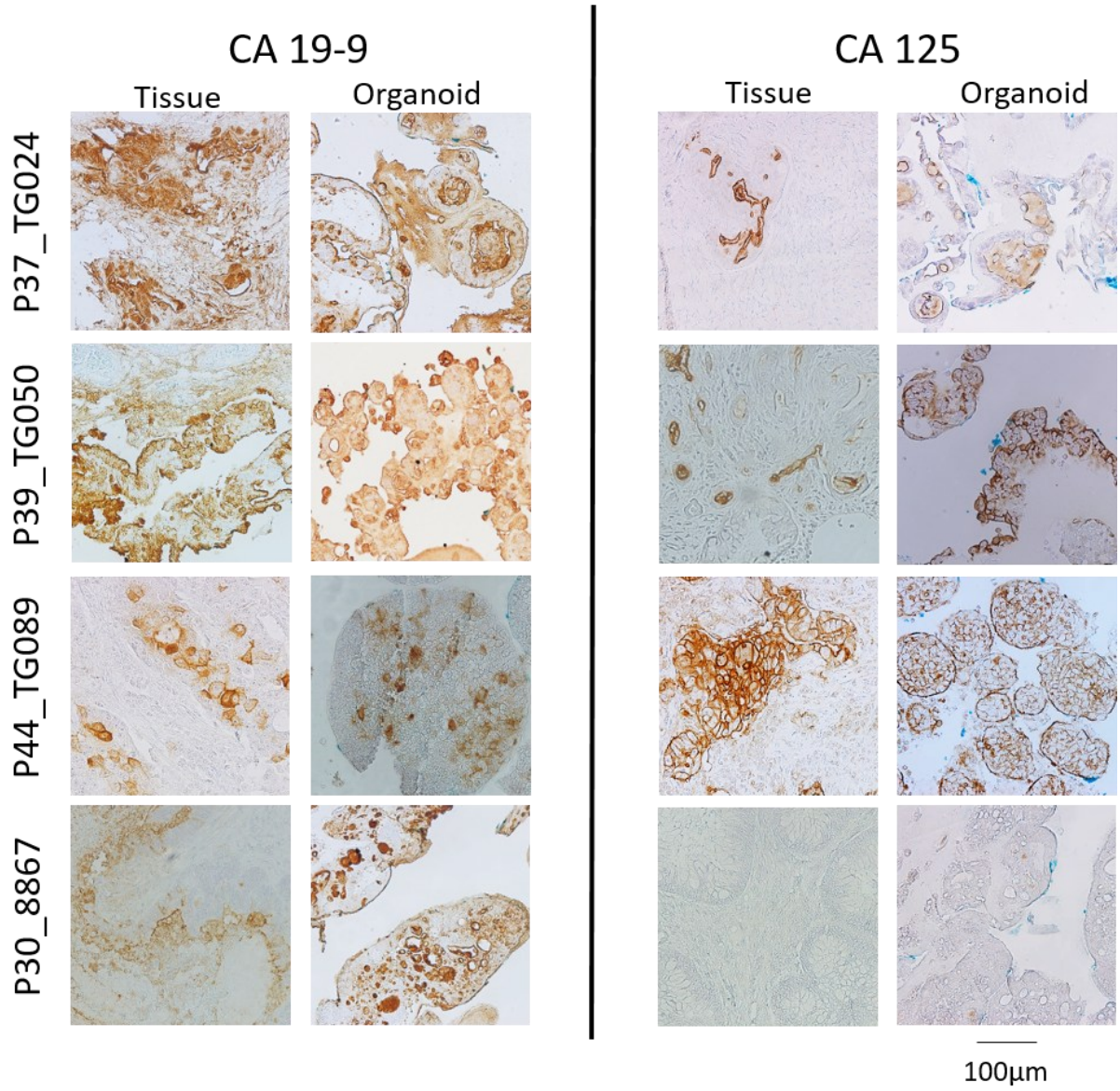

Figure 7: CA 19-9 and CA 125 expression by IHC in patient-derived organoids and their corresponding tumour tissues.

4.4.2. Organoids showed similar expression of potential therapeutic markers

In figure 8, MEK1/2 was positively expressed on the membrane of all organoid**s** and their corresponding tumour tissues. However, TG024 expressed MEK1/2 only partially. HER2 was positively expressed on the cell membrane of all organoid cells and their corresponding tumour tissues. Cyclin E1 was positively expressed on the cell membrane of all organoid cells and their corresponding tumour tissues. All organoids recapitulated the MEK1/2 expression pattern of their parent tumours. A congruent expression pattern for HER2 and Cyclin E1 was also observed between organoids and tumour tissues for all organoids and their parent tumours.

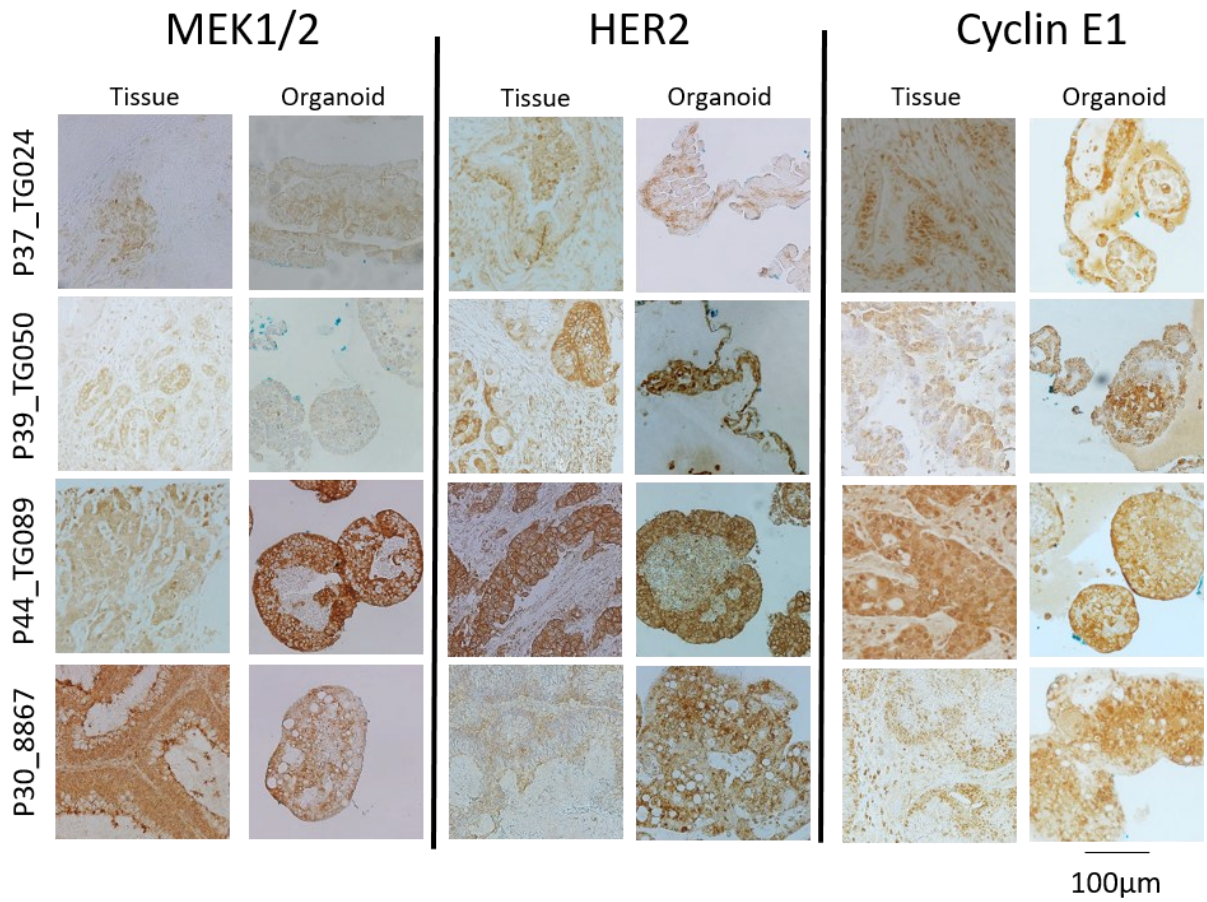

Figure 8: MEK1/2, HER2 and Cyclin E1 expression by IHC in patient-derived organoids and their corresponding tumour tissues.

The colorectal cancer cells are sensitive to Trametinib and therefore was used as a drug testing control. HT-29 was shown to be sensitive to Trametinib by Yamaguchi *et. al.* (76). HT-29 was IHC stained for the same proteins as the MOC tissues and organoids (figure 9). EpCAM, CK20, MEK1/2, HER2 and Cyclin E1 were positively expressed in HT-29. CA 19-9 was partially positively expressed in HT-29, while MUC1, CK7 and CA 125 were not expressed in HT-29. Opposite to MOC cell lines, HT-29 does not express MUC1, but does express high amounts of CK20. HT-29 showed the most similarities to cell line 8867 in protein expression.

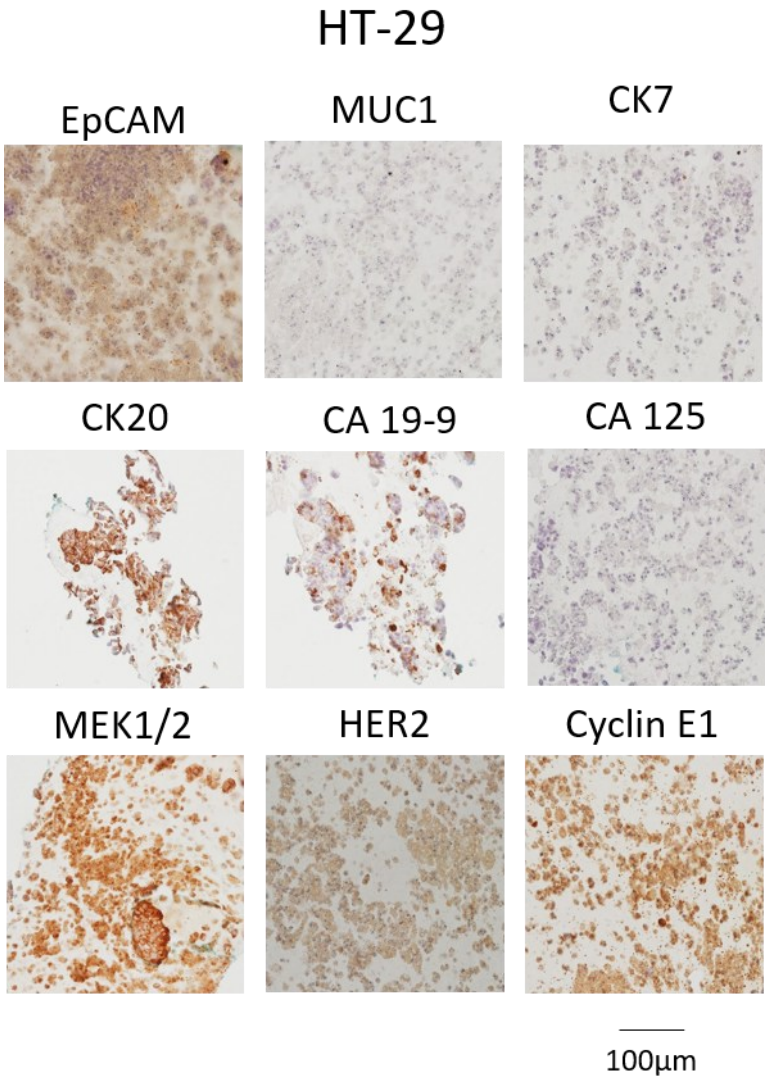

Figure 9: Commercial cell line HT-29 staining for all above-mentioned markers: EpCAM, MUC1, CK7, CK20, CA 19-9, CA 125, MEK1/2, HER2, and Cyclin E1.

Table 4 gives an overview of staining performed to compare the expression patterns of the patient-derived tissue and the organoids. Divergence was only found in MUC1 expression in TG024 and 8867. All other protein expressions were similar in tumour tissues and organoids. In both cases, MUC1 was partially expressed in tumour tissues, while it was expressed strongly in all cells in the organoids. All other protein expressions were similar in tumour tissues and organoids.

Table 4: Grading of IHC stainings comparing the patient-derived tissues with the organoids.

	TG024		TG050		TG089		8867		HT-29
	Tissue	Organoid	Tissue	Organoid	Tissue	Organoid	Tissue	Organoid	Organoid
EpCAM	+	+	+	+	+	+	+	+	+
MUC1	+/-	+	+	+	+	+	+/-	+	-
CK7	+/-	+/-	+/-	+/-	+	+	-	-	-
CK20	-	-	+/-	+/-	-	-	+/-	+/-	+
CA 19-9	+	+	+	+	+/-	+/-	+/-	+/-	+/-
CA 125	+/-	+/-	+/-	+/-	+	+	-	-	-
MEK1/2	+/-	+/-	+	+	+	+	+	+	+
HER2	+	+	+	+	+	+	+	+	+
Cyclin E1	+	+	+	+	+	+	+	+	+

+ = positive staining, +/- = partial positive staining, - = negative staining.

4.5. Different drug responses across cell lines in live-cell imaging

The cell lines showed varying sensitivity to both Carboplatin and Trametinib, see figure 10. At 150 µM, carboplatin showed minimal effect in TG089, moderate effect in TG050 and HT-29 and a strong effect in TG024 and 8867. Trametinib showed different efficacy in different cell lines. At 0.4 µM concentration, Trametinib showed minimal effect in TG024 and TG089, moderate effect in 8867 and a strong effect in TG050 and HT-29. Increasing the Trametinib concentration to 2 µM, then to 10 µM and 50 µM revealed an increasingly strong effect in TG024, TG050 and 8867, while TG089 still showed minimal effect and HT-29 had a strong effect regardless of the concentration of Trametinib (figure 10).

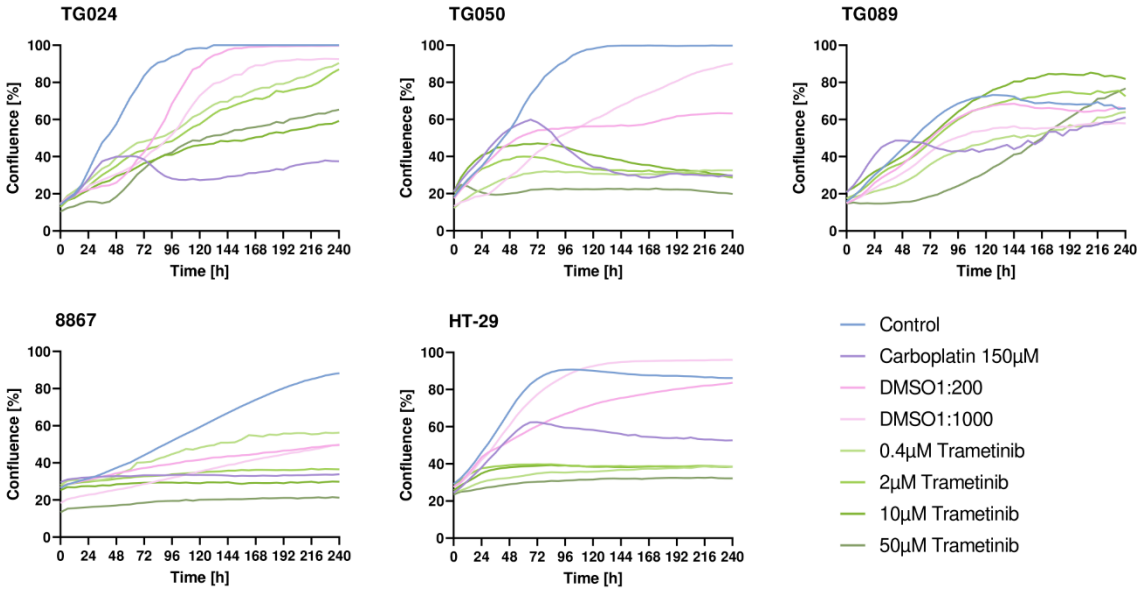

Figure 10: Response to Carboplatin and Trametinib treatment. Phase confluency is plotted against time in hours. DMSO was used as a control as Trametinib was dissolved in DMSO.

4.6. Different responses to cell viability versus cytotoxicity assay

To further assess the effects of Trametinib cell viability and cytotoxicity assays were. performed using fluorescent dyes. As shown in figure 11, Trametinib showed clear better antiproliferative effect than carboplatin in the control cell line HT-29 at all concentrations and slightly better effect in 8867 with higher concentrations, but not significant difference as carboplatin in TG024 and TG050. For TG089, both carboplatin and trametinib showed no antiproliferative effect except that Trametinib had an antiproliferative effect at the concentration of 50 µM. Regarding the cytotoxicity carboplatin and high doses (50 µM) of Trametinib showed effects across all MOC cell lines.

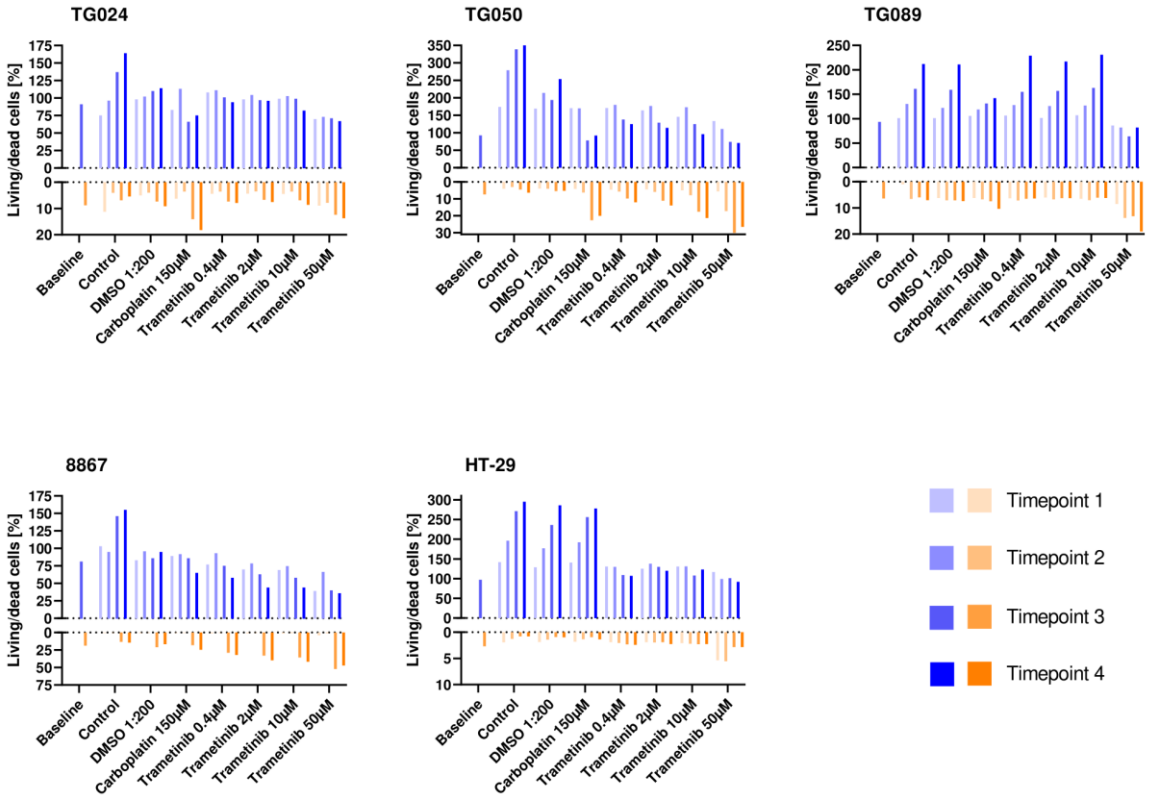

Figure 11: Comparative effects of Trametinib and Carboplatin on cell proliferation and cytotoxicity. Measurements were taken based on doubling times of the cell lines. They were performed every 24 hours for TG089 and HT-29, every 48 hours for TG024 and 8867, and every 72 hours for TG050. Cell viability is displayed in varying shades of purple, while cell toxicity is displayed in varying shades of orange.

4.7. Validation of drug treatment related markers

In order to validate the effects of Trametinib and explore its molecular mechanisms, organoids were treated with medium, 150µM Carboplatin or 10µM Trametinib after 5 days of seeding and processed to FFPE after 24 hours and 72 hours. As shown in figure 12, Trametinib showed only limited proliferation inhibition on day 1, but increased inhibitory effect on day 3 in TG050, 8867 and HT-29 – presented by a higher number of Ki67 positive cells at day 1 than at day 3. Carboplatin displayed also limited amount of proliferation inhibition on day 1 but increased inhibitory effects in day 3 in all cell lines. However, the effects of Trametinib on proliferation were stronger in the cell lines TG050, 8867 and HT-29.

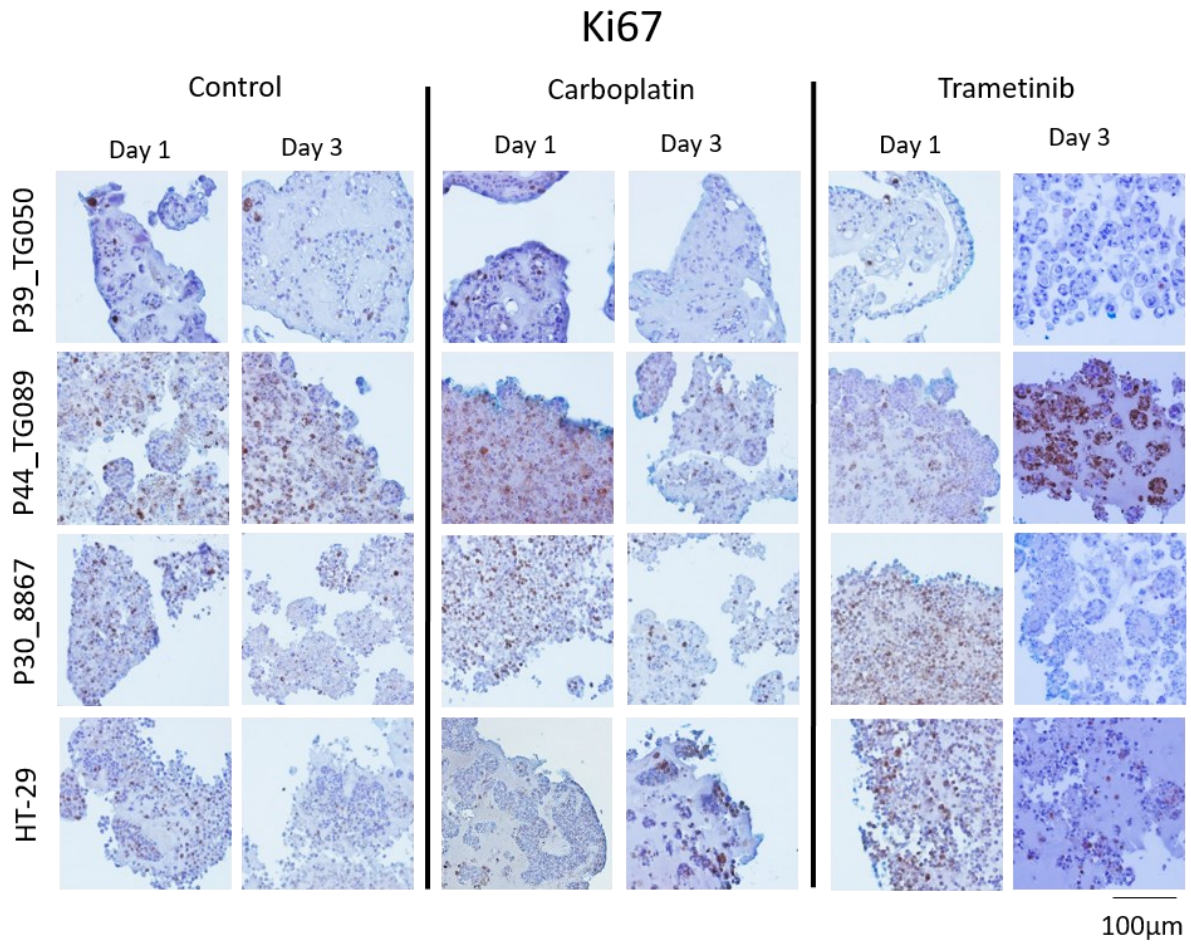

Figure 12: IHC staining of proliferation marker Ki67 in organoids of TG050, TG089, 8867 and HT-29 after 24 hours and 72 hours of treatment.

As shown in figure 13, Trametinib showed only limited apoptosis on day 1 and more apoptosis on day 3 in TG089 and 8867. In TG050 and HT-29 Trametinib caused no apoptosis in contrast to the control cells. Carboplatin displayed different levels of apoptosis depending on the cell line on day 1 but increased apoptotic effects in day 3 in all cell lines. The effects of carboplatin on apoptosis were stronger in all cell lines.

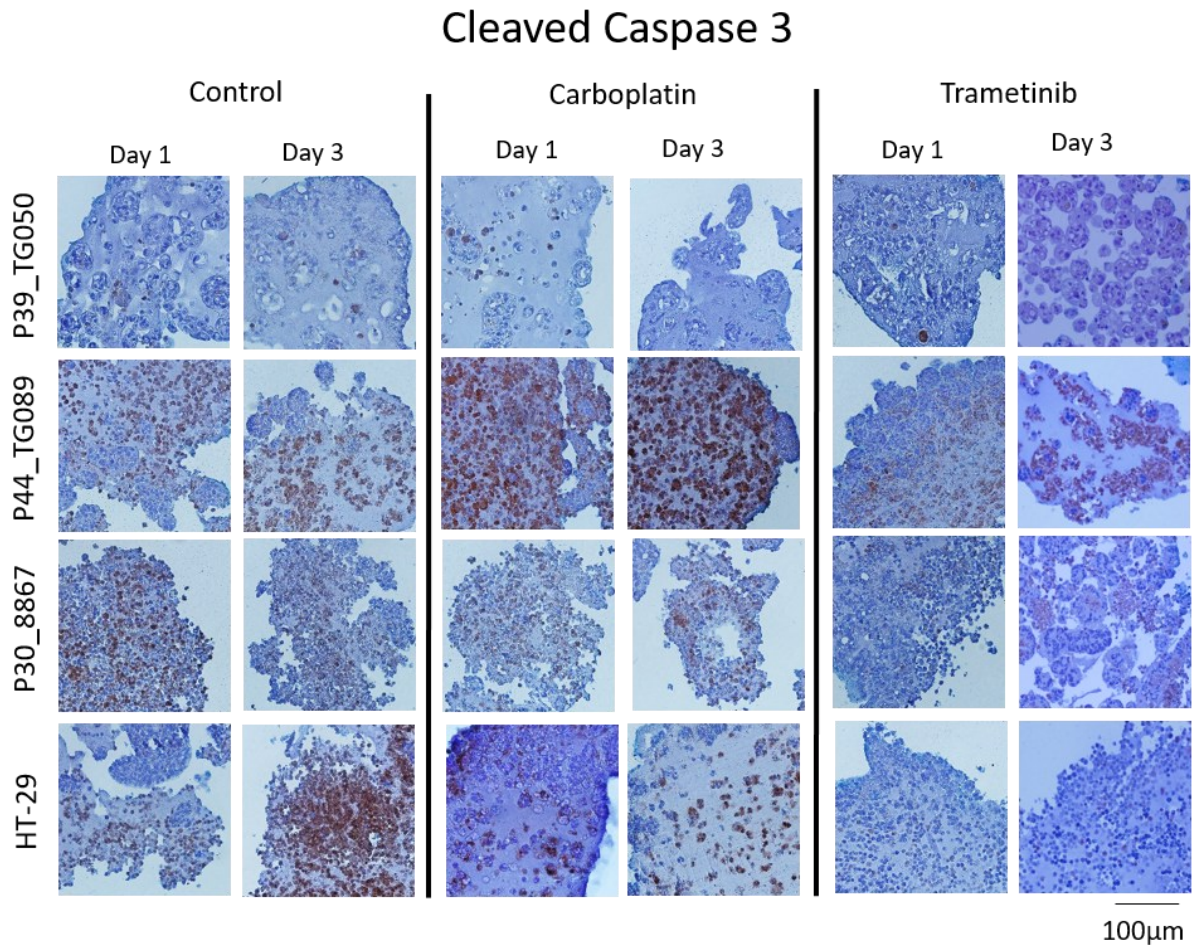

Figure 13: IHC staining of apoptosis marker cleaved caspase 3 in organoids of TG050, TG089, 8867 and HT-29 after 24 hours and 72 hours of treatment.

As shown in figure 14, Trametinib showed an instantaneous effect on c-fos on day 1 and no c-fos could be found on day 3 in TG050, 8867 and HT-29. In TG089 Trametinib showed only limited effect. Carboplatin showed no effect on c-fos expression all cell lines looked similar to the control. The effects of Trametinib on c-fos expression were proven in all cell lines.

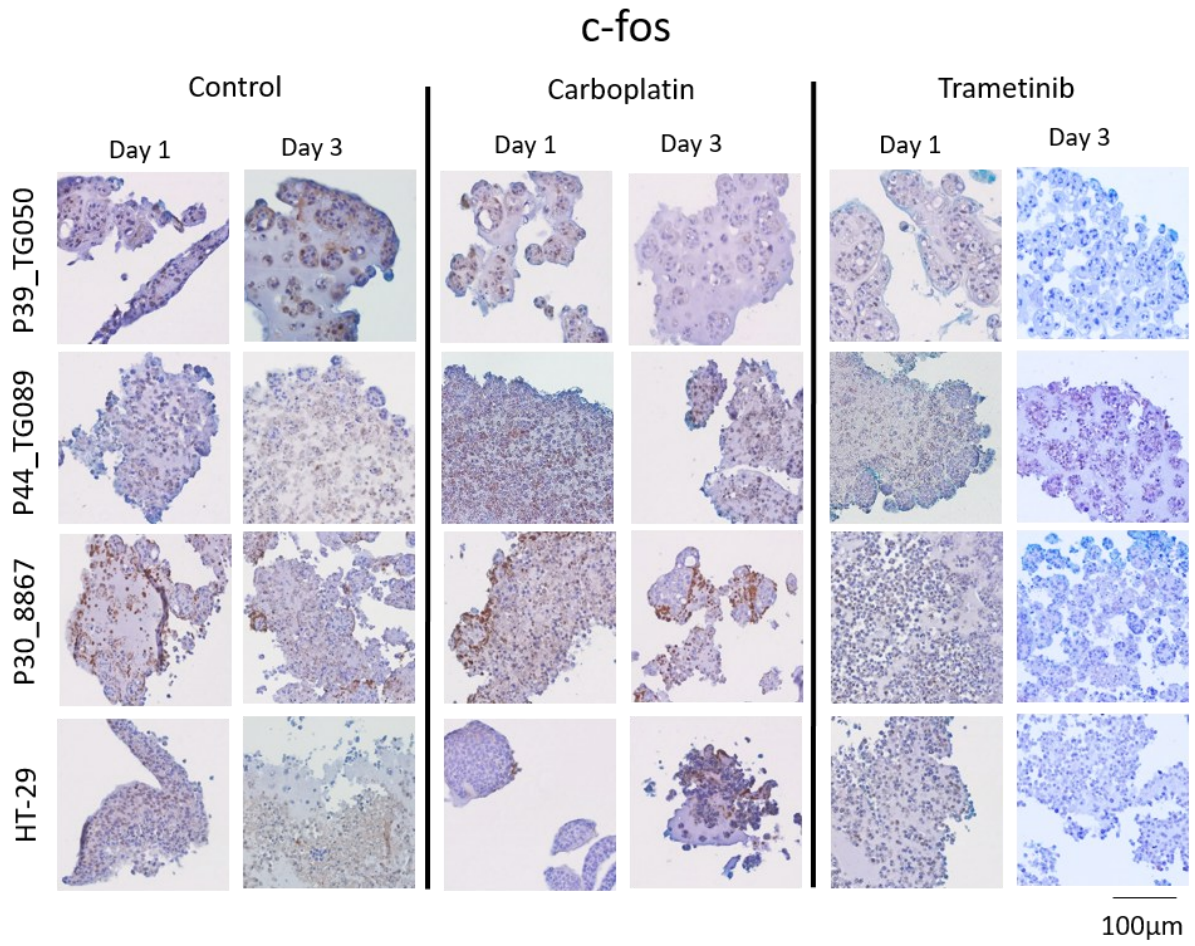

Figure 14: IHC staining of downstream marker c-fos in organoids of TG050, TG089, 8867 and HT-29 after 24 hours and 72 hours of treatment.

5. Discussion

MOC generally does not respond well to standard platinum-based chemotherapy and the survival rate of the patients is low once the disease becomes resistant to treatment. Unlike HGSOC, which may respond to platinum-based therapies, MOC often shows limited sensitivity, and treatment options are very limited after the first-line therapy fails (7, 8). Because of this, there is a strong need to explore alternative drug targets and drugs. Ideally, therapeutic targets should have several binding sites and the ability to be modulated by the drug (97). Drugs that are effective in cancer treatment should selectively target tumour cells, show consistent results across different tests and ideally cause decreased proliferation or induce apoptosis (98). In the case of targeted therapies, it is important that the drug targets are expressed in the tumour cells (99).

In this project, organoids were established using patient-derived MOC cell lines and the CRC cell line HT-29, which served as a positive control. These MOC organoids were then compared to the original tumor tissues and tested with trametinib to evaluate treatment effects across multiple assays including live imaging, cell viability, and IHC staining. The organoids closely resembled the tumors they were derived from, both in structure and protein expression. Interestingly, the HT-29 organoids showed an expression pattern of tumour specific biomarkers similar to the 8867 MOC line, which has an expansile histopathological sub-type. This indicates that CRC cells share certain characteristics with MOC, which was also discussed by Kelemen and Köbel in their review (100). The structural and molecular similarity between organoids and their original tumours highlights their potential as a model system for drug testing and validation (101).

For each of the tested cell lines, treatment effects were consistent in live-imaging, cell viability/ cytotoxicity assays and IHC staining. Reduced growth and viability observed in live imaging matched results from cell viability and cytotoxicity assay, and these were further supported by IHC staining for proliferation (Ki67) and apoptosis (cleaved caspase 3). This cross-validation strengthens confidence of the result of this study.

HT-29 acted as a positive control and showed strong MEK1/2 expression. It resulted minimal growth in the live imaging and cell viability/ cell toxicity assay under trametinib treatment, proving the efficacy of trametinib in this cell line. Even though trametinib reduces proliferation, it is not completely inhibited due to fast cell growth. There was nearly no cleaved caspase 3 expression after trametinib treatment and no expression of c-fos, suggesting that trametinib could have successfully blocked the MEK1/2 and thus inhibit the c-fos expression.

Interestingly, the individual cell lines showed different response treatment. For TG204, carboplatin was more effective than the MEK inhibitor trametinib in both live-imaging experiments and the cell viability/ cell toxicity assay. Even though TG024 had a *KRAS* mutation, which usually lead to an overactivation of the MAPK pathway, the lower expression of the MEK1/2 might be caused by other reasons and thus led to a less effect of the trametinib.

In comparison, in TG050 carboplatin was more effective in the cell viability/ cell toxicity assay, while trametinib was more effective in the live imaging. IHC staining of proliferation (Ki67) and apoptosis (cleaved caspase 3) markers revealed similar inhibition of both therapeutics on proliferation and more apoptosis by carboplatin. Overall, carboplatin at 150 µM and trametinib at 10 µM showed similar efficacy, with higher doses of trametinib, it was more effective. TG050 strongly expressed MEK1/2 in the tissue, while also harbouring a *KRAS* mutation, which suggests an overactive MAPK pathway and thereby could explain the observed trametinib efficacy.

TG089 was fast growing and the patient had a progressive disease. The chemotherapeutic treatments in the patient already showed therapeutic resistance presented by the increasing tumour markers during therapy and this was confirmed by live-imaging test. In both live-imaging test and 2D fluorescent tests, trametinib showed no inhibition of cell growth and carboplatin had little effect as well. TG089 also expressed MEK1/2 in the majority of cells but did not harbour a *KRAS* mutation. Instead, it harboured a *STK11* mutation, which activates the FOXO pathway and the MAPK pathway normally blocks FOXO(102, 103). TG089 is the only cell line in this project that was established after drug treatment in the patient, while the other three cell lines (TG024, TG050 and 8867) were established before the respective patients underwent chemotherapeutical treatment. Therefore, this cell line might have derived from the surviving, resistant cells and thus showed no response.

Live imaging for 8867 showed similar efficacy of both drugs, while the cell viability/ cell toxicity assay indicated trametinib to be slightly more effective. Staining of proliferation and apoptosis markers revealed a decreased proliferation under carboplatin treatment and no proliferation in trametinib after 72 hours of treatment, while carboplatin treatment showed more apoptosis than trametinib demonstrated by cleaved caspase 3 staining. 8867 had a high MEK1/2 expression and *KRAS* was mutated, potentially arguing for the trametinib efficacy.

Overall, the cell lines (except for TG089) showed no c-fos expression after trametinib treatment, indicating a successful inhibition of MEK1/2. In the cell viability/ cell toxicity assay a reduction in growth was observed after trametinib treatment, but only minimal increased in dead cells. This was supported by cleaved caspase 3, which was only minimally or not at all expression in the organoids after trametinib treatment. This suggested that trametinib might acts cytostatic which the state of the art literature also mentioned. Hartmann *et.al.*, George *et. al.* and Kurata *et. al.* showed the cytostatic effect of trametinib in melanoma cells, lymphoblastic leukaemia and thyroid cancer (104-106). TG050 and 8867 responded best to trametinib, likely due to their *KRAS* mutations and high MEK1/2 expression levels. TG024 was less responsive, while TG089 showed no response at all. Our results suggest that cell lines harbouring both a *KRAS* mutation and a high expression of MEK1/2 are responding more effectively to trametinib.

Every cell line had different response to trametinib, as well as to carboplatin. This is likely due to the heterogeneity of MOC, regarding their genetic alterations, histopathological subtypes and growth rate of the cancer. Targeted or personalized therapies could eventually administered based on the genetic alteration and/or target marker expression with the ultimate goal to prolong disease free survival of the patients.

In conclusion, the findings in this study suggest that MEK inhibitor trametinib could be useful for treating a subset of MOC patients—particularly those with both high MEK1/2 expression and possibly *KRAS* mutations. Since the drug appears to be cytostatic, it might be more effective in combination therapies rather than as a standalone treatment. Further testing, especially in patient-derived organoids, is needed to confirm these observations and better understand resistance mechanisms.

6. Bibliography

1. Seidman JD, Horkayne-Szakaly I, Haiba M, Boice CR, Kurman RJ, Ronnett BM. The histologic type and stage distribution of ovarian carcinomas of surface epithelial origin. Int J Gynecol Pathol. 2004;23(1):41-4.

2. Morgan RJ, Jr., Armstrong DK, Alvarez RD, Bakkum-Gamez JN, Behbakht K, Chen LM, et al. Ovarian Cancer, Version 1.2016, NCCN Clinical Practice Guidelines in Oncology. J Natl Compr Canc Netw. 2016;14(9):1134-63.

3. Seidman JD, Soslow RA, Vang R, Berman JJ, Stoler MH, Sherman ME, et al. Borderline ovarian tumors: diverse contemporary viewpoints on terminology and diagnostic criteria with illustrative images. Hum Pathol. 2004;35(8):918-33.

4. Kurnit KC, Frumovitz M. Primary mucinous ovarian cancer: options for surgery and chemotherapy. Int J Gynecol Cancer. 2022;32(11):1455-62.

5. Morice P, Gouy S, Leary A. Mucinous Ovarian Carcinoma. N Engl J Med. 2019;380(13):1256-66.

6. Gonzalez-Martin A, Harter P, Leary A, Lorusso D, Miller RE, Pothuri B, et al. Newly diagnosed and relapsed epithelial ovarian cancer: ESMO Clinical Practice Guideline for diagnosis, treatment and follow-up. Ann Oncol. 2023;34(10):833-48.

7. Peres LC, Cushing-Haugen KL, Kobel M, Harris HR, Berchuck A, Rossing MA, et al. Invasive Epithelial Ovarian Cancer Survival by Histotype and Disease Stage. J Natl Cancer Inst. 2019;111(1):60-8.

8. Zaino RJ, Brady MF, Lele SM, Michael H, Greer B, Bookman MA. Advanced stage mucinous adenocarcinoma of the ovary is both rare and highly lethal: a Gynecologic Oncology Group study. Cancer. 2011;117(3):554-62.

9. Xu W, Rush J, Rickett K, Coward JI. Mucinous ovarian cancer: A therapeutic review. Crit Rev Oncol Hematol. 2016;102:26-36.

10. Lu Z, Chen J. [Introduction of WHO classification of tumours of female reproductive organs, fourth edition]. Zhonghua Bing Li Xue Za Zhi. 2014;43(10):649-50.

11. Lee KR, Scully RE. Mucinous tumors of the ovary: a clinicopathologic study of 196 borderline tumors (of intestinal type) and carcinomas, including an evaluation of 11 cases with 'pseudomyxoma peritonei'. Am J Surg Pathol. 2000;24(11):1447-64.

12. Muyldermans K, Moerman P, Amant F, Leunen K, Neven P, Vergote I. Primary invasive mucinous ovarian carcinoma of the intestinal type: importance of the expansile versus infiltrative type in predicting recurrence and lymph node metastases. Eur J Cancer. 2013;49(7):1600-8.

13. Gouy S, Saidani M, Maulard A, Bach-Hamba S, Bentivegna E, Leary A, et al. Characteristics and Prognosis of Stage I Ovarian Mucinous Tumors According to Expansile or Infiltrative Type. Int J Gynecol Cancer. 2018;28(3):493-9.

14. Meagher NS, Hamilton P, Milne K, Thornton S, Harris B, Weir A, et al. Profiling the immune landscape in mucinous ovarian carcinoma. Gynecol Oncol. 2023;168:23-31.

15. Mackenzie R, Kommoss S, Winterhoff BJ, Kipp BR, Garcia JJ, Voss J, et al. Targeted deep sequencing of mucinous ovarian tumors reveals multiple overlapping RAS-pathway activating mutations in borderline and cancerous neoplasms. BMC Cancer. 2015;15:415.

16. Chang KL, Lee MY, Chao WR, Han CP. The status of Her2 amplification and Kras mutations in mucinous ovarian carcinoma. Hum Genomics. 2016;10(1):40.

17. Ryland GL, Hunter SM, Doyle MA, Caramia F, Li J, Rowley SM, et al. Mutational landscape of mucinous ovarian carcinoma and its neoplastic precursors. Genome Med. 2015;7(1):87.

18. Bartl T, Alberts A, Papadopoulos SC, Wolf A, Muellauer L, Hofstetter G, et al. Biomarkers for checkpoint inhibitor therapy in mucinous epithelial ovarian cancer. Int J Gynecol Cancer. 2023;33(9):1419-26.

19. Martowicz A, Seeber A, Untergasser G. The role of EpCAM in physiology and pathology of the epithelium. Histol Histopathol. 2016;31(4):349-55.

20. Trzpis M, Popa ER, McLaughlin PM, van Goor H, Timmer A, Bosman GW, et al. Spatial and temporal expression patterns of the epithelial cell adhesion molecule (EpCAM/EGP-2) in developing and adult kidneys. Nephron Exp Nephrol. 2007;107(4):e119-31.

21. Baeuerle PA, Gires O. EpCAM (CD326) finding its role in cancer. Br J Cancer. 2007;96(3):417-23.

22. Gastl G, Spizzo G, Obrist P, Dunser M, Mikuz G. Ep-CAM overexpression in breast cancer as a predictor of survival. Lancet. 2000;356(9246):1981-2.

23. Kalluri R. EMT: when epithelial cells decide to become mesenchymal-like cells. J Clin Invest. 2009;119(6):1417-9.

24. Litvinov SV, Balzar M, Winter MJ, Bakker HA, Briaire-de Bruijn IH, Prins F, et al. Epithelial cell adhesion molecule (Ep-CAM) modulates cell-cell interactions mediated by classic cadherins. J Cell Biol. 1997;139(5):1337-48.

25. Deng J, Wang L, Chen H, Li L, Ma Y, Ni J, et al. The role of tumour-associated MUC1 in epithelial ovarian cancer metastasis and progression. Cancer Metastasis Rev. 2013;32(3-4):535-51.

26. Uhlen M, Fagerberg L, Hallstrom BM, Lindskog C, Oksvold P, Mardinoglu A, et al. Proteomics. Tissue-based map of the human proteome. Science. 2015;347(6220):1260419.

27. Yamamoto M, Bharti A, Li Y, Kufe D. Interaction of the DF3/MUC1 breast carcinoma-associated antigen and beta-catenin in cell adhesion. J Biol Chem. 1997;272(19):12492-4.

28. Li Y, Yu WH, Ren J, Chen W, Huang L, Kharbanda S, et al. Heregulin targets gamma-catenin to the nucleolus by a mechanism dependent on the DF3/MUC1 oncoprotein. Mol Cancer Res. 2003;1(10):765-75.

29. Dong Y, Walsh MD, Cummings MC, Wright RG, Khoo SK, Parsons PG, et al. Expression of MUC1 and MUC2 mucins in epithelial ovarian tumours. J Pathol. 1997;183(3):311-7.

30. Gaemers IC, Vos HL, Volders HH, van der Valk SW, Hilkens J. A stat-responsive element in the promoter of the episialin/MUC1 gene is involved in its overexpression in carcinoma cells. J Biol Chem. 2001;276(9):6191-9.

31. Hughes OD, Bishop MC, Perkins AC, Wastie ML, Denton G, Price MR, et al. Targeting superficial bladder cancer by the intravesical administration of copper-67-labeled anti-MUC1 mucin monoclonal antibody C595. J Clin Oncol. 2000;18(2):363-70.

32. Schroeder JA, Adriance MC, Thompson MC, Camenisch TD, Gendler SJ. MUC1 alters beta-catenin-dependent tumor formation and promotes cellular invasion. Oncogene. 2003;22(9):1324-32.

33. Dum D, Menz A, Volkel C, De Wispelaere N, Hinsch A, Gorbokon N, et al. Cytokeratin 7 and cytokeratin 20 expression in cancer: A tissue microarray study on 15,424 cancers. Exp Mol Pathol. 2022;126:104762.

34. Park SY, Kim HS, Hong EK, Kim WH. Expression of cytokeratins 7 and 20 in primary carcinomas of the stomach and colorectum and their value in the differential diagnosis of metastatic carcinomas to the ovary. Hum Pathol. 2002;33(11):1078-85.

35. Vang R, Gown AM, Barry TS, Wheeler DT, Yemelyanova A, Seidman JD, et al. Cytokeratins 7 and 20 in primary and secondary mucinous tumors of the ovary: analysis of coordinate immunohistochemical expression profiles and staining distribution in 179 cases. Am J Surg Pathol. 2006;30(9):1130-9.

36. Pavai S, Yap SF. The clinical significance of elevated levels of serum CA 19-9. Med J Malaysia. 2003;58(5):667-72.

37. Kyung MS, Choi JS, Hong SH, Kim HS. Elevated CA 19-9 levels in mature cystic teratoma of the ovary. Int J Biol Markers. 2009;24(1):52-6.

38. Cho DH, Lee JH, Oh BC. Unusual presentation of retroperitoneal leiomyosarcoma mimicking an adnexal tumor with highly elevated serum CA-19-9. Obstet Gynecol Sci. 2014;57(1):77-81.

39. Visser CE, Brouwer-Steenbergen JJ, Betjes MG, Koomen GC, Beelen RH, Krediet RT. Cancer antigen 125: a bulk marker for the mesothelial mass in stable peritoneal dialysis patients. Nephrol Dial Transplant. 1995;10(1):64-9.

40. Berek JS, Crum C, Friedlander M. Cancer of the ovary, fallopian tube, and peritoneum. Int J Gynaecol Obstet. 2015;131 Suppl 2:S111-22.

41. Gadducci A, Ferdeghini M, Prontera C, Moretti L, Mariani G, Bianchi R, et al. The concomitant determination of different tumor markers in patients with epithelial ovarian cancer and benign ovarian masses: relevance for differential diagnosis. Gynecol Oncol. 1992;44(2):147-54.

42. Bast RC, Jr., Klug TL, St John E, Jenison E, Niloff JM, Lazarus H, et al. A radioimmunoassay using a monoclonal antibody to monitor the course of epithelial ovarian cancer. N Engl J Med. 1983;309(15):883-7.

43. Zorn KK, Tian C, McGuire WP, Hoskins WJ, Markman M, Muggia FM, et al. The prognostic value of pretreatment CA 125 in patients with advanced ovarian carcinoma: a Gynecologic Oncology Group study. Cancer. 2009;115(5):1028-35.

44. Estep AL, Palmer C, McCormick F, Rauen KA. Mutation analysis of BRAF, MEK1 and MEK2 in 15 ovarian cancer cell lines: implications for therapy. PLoS One. 2007;2(12):e1279.

45. Han R, Madariaga A, Gonzalez-Ochoa E, Smith AC, Wang L, Lheureux S, et al. HER2-low and Overexpression in Mucinous Ovarian Cancer: Analysis of ASCO/CAP and ToGA Immunohistochemical Scoring. Int J Gynecol Pathol. 2024;43(3):275-83.

46. Jain A, Ryan PD, Seiden MV. Metastatic mucinous ovarian cancer and treatment decisions based on histology and molecular markers rather than the primary location. J Natl Compr Canc Netw. 2012;10(9):1076-80.

47. McAlpine JN, Wiegand KC, Vang R, Ronnett BM, Adamiak A, Kobel M, et al. HER2 overexpression and amplification is present in a subset of ovarian mucinous carcinomas and can be targeted with trastuzumab therapy. BMC Cancer. 2009;9:433.

48. Pang W, Li Y, Guo W, Shen H. Cyclin E: a potential treatment target to reverse cancer chemoresistance by regulating the cell cycle. Am J Transl Res. 2020;12(9):5170-87.

49. Scholzen T, Gerdes J. The Ki-67 protein: from the known and the unknown. J Cell Physiol. 2000;182(3):311-22.

50. Yerushalmi R, Woods R, Ravdin PM, Hayes MM, Gelmon KA. Ki67 in breast cancer: prognostic and predictive potential. Lancet Oncol. 2010;11(2):174-83.

51. Kumar S. Regulation of caspase activation in apoptosis: implications in pathogenesis and treatment of disease. Clin Exp Pharmacol Physiol. 1999;26(4):295-303.

52. O'Donovan N, Crown J, Stunell H, Hill AD, McDermott E, O'Higgins N, et al. Caspase 3 in breast cancer. Clin Cancer Res. 2003;9(2):738-42.

53. McIlwain DR, Berger T, Mak TW. Caspase functions in cell death and disease. Cold Spring Harb Perspect Biol. 2013;5(4):a008656.

54. Loro L, Vintermyr OK, Johannessen AC. Apoptosis in normal and diseased oral tissues. Oral Dis. 2005;11(5):274-87.

55. Mahner S, Baasch C, Schwarz J, Hein S, Wolber L, Janicke F, et al. C-Fos expression is a molecular predictor of progression and survival in epithelial ovarian carcinoma. Br J Cancer. 2008;99(8):1269-75.
56. Wang X, Tao X, Chen P, Jiang P, Li W, Chang H, et al. MEK inhibition prevents CAR-T cell exhaustion and differentiation via downregulation of c-Fos and JunB. Signal Transduct Target Ther. 2024;9(1):293.
57. Hess V, A'Hern R, Nasiri N, King DM, Blake PR, Barton DP, et al. Mucinous epithelial ovarian cancer: a separate entity requiring specific treatment. J Clin Oncol. 2004;22(6):1040-4.
58. Pectasides D, Fountzilas G, Aravantinos G, Kalofonos HP, Efstathiou E, Salamalekis E, et al. Advanced stage mucinous epithelial ovarian cancer: the Hellenic Cooperative Oncology Group experience. Gynecol Oncol. 2005;97(2):436-41.
59. Sato S, Itamochi H, Kigawa J, Oishi T, Shimada M, Sato S, et al. Combination chemotherapy of oxaliplatin and 5-fluorouracil may be an effective regimen for mucinous adenocarcinoma of the ovary: a potential treatment strategy. Cancer Sci. 2009;100(3):546-51.
60. Kurnit KC, Sinno AK, Fellman BM, Varghese A, Stone R, Sood AK, et al. Effects of Gastrointestinal-Type Chemotherapy in Women With Ovarian Mucinous Carcinoma. Obstet Gynecol. 2019;134(6):1253-9.
61. Information. NCfB. Compound Summary for CID 10339178, Carboplatin PubChem Accessed 2 April, 2025.
62. Pisano C, Greggi S, Tambaro R, Losito S, Iodice F, Di Maio M, et al. Activity of chemotherapy in mucinous epithelial ovarian cancer: a retrospective study. Anticancer Res. 2005;25(5):3501-5.
63. Information NCfB. PubChem Compound Summary for CID 36314, Paclitaxel. PubChem. Acessed 2 April, 2025.
64. Information. NCfB. PubChem Compound Summary for Bevacizumab. PubChem. Accessed 2 April, 2025.
65. Tarumi Y, Mori T, Matsushima H, Kokabu T, Tsuchiya H, Kitawaki J. Long-term survival with bevacizumab in heavily pretreated and platinum-resistant mucinous ovarian cancer: A case report. J Obstet Gynaecol Res. 2018;44(2):347-51.
66. Winer I, Buckanovich RJ. A case of progressive mucinous ovarian cancer of low malignant potential responsive to biologic therapy with Bevacizumab. Gynecol Oncol. 2010;116(3):578-9.
67. Information NCfB. PubChem Compound Summary for CID 443939, Doxorubicin Hydrochloride. **PubChem**. Accessed 2 April, 2025.
68. Pignata S, Ferrandina G, Scarfone G, Scollo P, Odicino F, Cormio G, et al. Activity of chemotherapy in mucinous ovarian cancer with a recurrence free interval of more than 6 months: results from the SOCRATES retrospective study. BMC Cancer. 2008;8:252.

69. Lowenstein EJ, Daly RJ, Batzer AG, Li W, Margolis B, Lammers R, et al. The SH2 and SH3 domain-containing protein GRB2 links receptor tyrosine kinases to ras signaling. Cell. 1992;70(3):431-42.

70. Morrison DK. MAP kinase pathways. Cold Spring Harb Perspect Biol. 2012;4(11).

71. Chang L, Karin M. Mammalian MAP kinase signalling cascades. Nature. 2001;410(6824):37-40.

72. Inaba K, Oda K, Aoki K, Sone K, Ikeda Y, Miyasaka A, et al. Synergistic antitumor effects of combination PI3K/mTOR and MEK inhibition (SAR245409 and pimasertib) in mucinous ovarian carcinoma cells by fluorescence resonance energy transfer imaging. Oncotarget. 2016;7(20):29577-91.

73. Gonzalez-Del Pino GL, Li K, Park E, Schmoker AM, Ha BH, Eck MJ. Allosteric MEK inhibitors act on BRAF/MEK complexes to block MEK activation. Proc Natl Acad Sci U S A. 2021;118(36).

74. Information NCfB. PubChem Compound Summary for CID 11707110, Trametinib. PubChem. Accessed 2 April, 2025.

75. Lorusso PM, Adjei AA, Varterasian M, Gadgeel S, Reid J, Mitchell DY, et al. Phase I and pharmacodynamic study of the oral MEK inhibitor CI-1040 in patients with advanced malignancies. J Clin Oncol. 2005;23(23):5281-93.

76. Yamaguchi T, Kakefuda R, Tajima N, Sowa Y, Sakai T. Antitumor activities of JTP-74057 (GSK1120212), a novel MEK1/2 inhibitor, on colorectal cancer cell lines in vitro and in vivo. Int J Oncol. 2011;39(1):23-31.

77. SelleckChem. Trametinib (GSK1120212) Accessed 7 April, 2025 [Available from: https://www.selleckchem.com/datasheet/gsk1120212-jtp-74057-S267313-DataSheet.html.

78. Solit DB, Garraway LA, Pratilas CA, Sawai A, Getz G, Basso A, et al. BRAF mutation predicts sensitivity to MEK inhibition. Nature. 2006;439(7074):358-62.

79. Liu S, Zou Q, Chen JP, Yao X, Guan P, Liang W, et al. Targeting enhancer reprogramming to mitigate MEK inhibitor resistance in preclinical models of advanced ovarian cancer. J Clin Invest. 2021;131(20).

80. Gilmartin AG, Bleam MR, Groy A, Moss KG, Minthorn EA, Kulkarni SG, et al. GSK1120212 (JTP-74057) is an inhibitor of MEK activity and activation with favorable pharmacokinetic properties for sustained in vivo pathway inhibition. Clin Cancer Res. 2011;17(5):989-1000.

81. Schubbert S, Shannon K, Bollag G. Hyperactive Ras in developmental disorders and cancer. Nat Rev Cancer. 2007;7(4):295-308.

82. Infante JR, Fecher LA, Falchook GS, Nallapareddy S, Gordon MS, Becerra C, et al. Safety, pharmacokinetic, pharmacodynamic, and efficacy data for the oral MEK inhibitor trametinib: a phase 1 dose-escalation trial. Lancet Oncol. 2012;13(8):773-81.

83. Beaufort CM, Helmijr JC, Piskorz AM, Hoogstraat M, Ruigrok-Ritstier K, Besselink N, et al. Ovarian cancer cell line panel (OCCP): clinical importance of in vitro morphological subtypes. PLoS One. 2014;9(9):e103988.

84. Chow T, Humble W, Lucarelli E, Onofrillo C, Choong PF, Di Bella C, et al. Feasibility and barriers to rapid establishment of patient-derived primary osteosarcoma cell lines in clinical management. iScience. 2024;27(9):110251.

85. Richter M, Piwocka O, Musielak M, Piotrowski I, Suchorska WM, Trzeciak T. From Donor to the Lab: A Fascinating Journey of Primary Cell Lines. Front Cell Dev Biol. 2021;9:711381.

86. Masters JR. Human cancer cell lines: fact and fantasy. Nat Rev Mol Cell Biol. 2000;1(3):233-6.

87. Ben-David U, Siranosian B, Ha G, Tang H, Oren Y, Hinohara K, et al. Genetic and transcriptional evolution alters cancer cell line drug response. Nature. 2018;560(7718):325-30.

88. Domcke S, Sinha R, Levine DA, Sander C, Schultz N. Evaluating cell lines as tumour models by comparison of genomic profiles. Nat Commun. 2013;4:2126.

89. Hidalgo M, Amant F, Biankin AV, Budinska E, Byrne AT, Caldas C, et al. Patient-derived xenograft models: an emerging platform for translational cancer research. Cancer Discov. 2014;4(9):998-1013.

90. Byrne AT, Alferez DG, Amant F, Annibali D, Arribas J, Biankin AV, et al. Interrogating open issues in cancer precision medicine with patient-derived xenografts. Nat Rev Cancer. 2017;17(4):254-68.

91. Cybulska P, Stewart JM, Sayad A, Virtanen C, Shaw PA, Clarke B, et al. A Genomically Characterized Collection of High-Grade Serous Ovarian Cancer Xenografts for Preclinical Testing. Am J Pathol. 2018;188(5):1120-31.

92. Drost J, Clevers H. Organoids in cancer research. Nat Rev Cancer. 2018;18(7):407-18.

93. Weiswald LB, Bellet D, Dangles-Marie V. Spherical cancer models in tumor biology. Neoplasia. 2015;17(1):1-15.

94. Graham O, Rodriguez J, van Biljon L, Fashemi B, Graham E, Fuh K, et al. Generation and Culturing of High-Grade Serous Ovarian Cancer Patient-Derived Organoids. J Vis Exp. 2023(191).

95. Nanki Y, Chiyoda T, Hirasawa A, Ookubo A, Itoh M, Ueno M, et al. Patient-derived ovarian cancer organoids capture the genomic profiles of primary tumours applicable for drug sensitivity and resistance testing. Sci Rep. 2020;10(1):12581.

96. John G Tate SB, Harry C Jubb, Zbyslaw Sondka, David M Beare, Nidhi Bindal, Harry Boutselakis, Charlotte G Cole, Celestino Creatore, Elisabeth Dawson, Peter Fish, Bhavana Harsha, Charlie Hathaway, Steve C Jupe, Chai Yin Kok, Kate Noble, Laura Ponting, Christopher C Ramshaw, Claire E Rye, Helen E Speedy, Ray Stefancsik, Sam L Thompson, Shicai Wang, Sari Ward, Peter J Campbell, Simon A Forbes, COSMIC: the Catalogue Of Somatic Mutations In Cancer, Nucleic Acids Research, Volume 47, Issue D1, 08 January 2019, Pages D941–D947, https://doi.org/10.1093/nar/gky1015, https://cancer.sanger.ac.uk/cell_lines/sample/overview?id=905939#muts.

97. Gashaw I, Ellinghaus P, Sommer A, Asadullah K. What makes a good drug target? Drug Discov Today. 2012;17 Suppl:S24-30.

98. Shuel SL. Targeted cancer therapies: Clinical pearls for primary care. Can Fam Physician. 2022;68(7):515-8.

99. Min HY, Lee HY. Molecular targeted therapy for anticancer treatment. Exp Mol Med. 2022;54(10):1670-94.

100. Kelemen LE, Kobel M. Mucinous carcinomas of the ovary and colorectum: different organ, same dilemma. Lancet Oncol. 2011;12(11):1071-80.

101. Xu H, Jiao D, Liu A, Wu K. Tumor organoids: applications in cancer modeling and potentials in precision medicine. J Hematol Oncol. 2022;15(1):58.

102. Kanehisa M, Goto S. KEGG: kyoto encyclopedia of genes and genomes. Nucleic Acids Res. 2000;28(1):27-30.

103. Glauser DA, Schlegel W. The emerging role of FOXO transcription factors in pancreatic beta cells. J Endocrinol. 2007;193(2):195-207.

104. Kurata K, Onoda N, Noda S, Kashiwagi S, Asano Y, Hirakawa K, et al. Growth arrest by activated BRAF and MEK inhibition in human anaplastic thyroid cancer cells. Int J Oncol. 2016;49(6):2303-8.

105. George AA, Paz H, Fei F, Kirzner J, Kim YM, Heisterkamp N, et al. Phosphoflow-Based Evaluation of Mek Inhibitors as Small-Molecule Therapeutics for B-Cell Precursor Acute Lymphoblastic Leukemia. PLoS One. 2015;10(9):e0137917.

106. Hartman ML, Rozanski M, Osrodek M, Zalesna I, Czyz M. Vemurafenib and trametinib reduce expression of CTGF and IL-8 in (V600E)BRAF melanoma cells. Lab Invest. 2017;97(2):217-27.

7. Addendum

7.1. Index of Figures

7.2. Index of Tables